Simulated Arctic Ocean Freshwater Budgets in the Twentieth and Twenty-First Centuries

MARIKA M. HOLLAND

National Center for Atmospheric Research, Boulder, Colorado*

JOEL FINNIS

Cooperative Institute for Research in Environmental Sciences, University of Colorado, Boulder, Colorado

MARK C. SERREZE

National Snow and Ice Data Center, University of Colorado, Boulder, Colorado

(Manuscript received 6 September 2005, in final form 25 April 2006)

ABSTRACT

The Arctic Ocean freshwater budgets in climate model integrations of the twentieth and twenty-first century are examined. An ensemble of six members of the Community Climate System Model version 3 (CCSM3) is used for the analysis, allowing the anthropogenically forced trends over the integration length to be assessed. Mechanisms driving trends in the budgets are diagnosed, and the implications of changes in the Arctic–North Atlantic exchange on the Labrador Sea and Greenland–Iceland–Norwegian (GIN) Seas properties are discussed. Over the twentieth and the twenty-first centuries, the Arctic freshens as a result of increased river runoff, net precipitation, and decreased ice growth. For many of the budget terms, the maximum 50-yr trends in the time series occur from approximately 1975 to 2025, suggesting that we are currently in the midst of large Arctic change. The total freshwater exchange between the Arctic and North Atlantic increases over the twentieth and twenty-first centuries with decreases in ice export more than compensated for by an increase in the liquid freshwater export. Changes in both the liquid and solid (ice) Fram Strait freshwater fluxes are transported southward by the East Greenland Current and partially removed from the GIN Seas. Nevertheless, reductions in GIN sea ice melt do result from the reduced Fram Strait transport and account for the largest term in the changing ocean surface freshwater fluxes in this region. This counteracts the increased ocean stability due to the warming climate and helps to maintain GIN sea deep-water formation.

1. Introduction

The hydrologic cycle of high northern latitudes is of significance because even small changes in the freshwater budget of the Arctic may influence ocean circulation, which can in turn affect the global climate (Broecker 1997; Broecker et al. 1985). The primary freshwater inputs to the Arctic Ocean are river discharge, chiefly from the drainages of the Ob, Yenesei, Lena, and Mackenzie; an import of fairly low salinity water through the Bering Strait; and net precipitation over the Arctic Ocean itself. There are two primary freshwater sinks, both representing flows to the North Atlantic. The first is a transport through Fram Strait and then along the eastern coast of Greenland via the East Greenland Current (EGC). The EGC transports sea ice as well as surface, intermediate, and deep water. The other primary sink is through the narrow, complex channels of the Canadian Arctic Archipelago (CAA), primarily as liquid water (e.g., Carmack 2000).

The Greenland–Iceland–Norwegian (GIN) and Labrador Seas are the primary regions affected by the freshwater transport from the Arctic. Additionally, they are major deep-water formation sites for the global

* The National Center for Atmospheric Research is sponsored by the National Science Foundation.

Corresponding author address: Marika M. Holland, National Center for Atmospheric Research, P.O. Box 3000, Boulder, CO 80307.
E-mail: mholland@ucar.edu

ocean. It appears that these regions may be delicately poised in their ability to sustain convection (Aagaard and Carmack 1989). Because density is largely a function of salinity at low temperatures, a moderate freshening of the surface waters of the North Atlantic could impact deep-water formation there. Through this impact, variations in Arctic–North Atlantic freshwater exchange can modify the global thermohaline circulation (THC). Observations suggest that this indeed took place during the Great Salinity Anomaly (GSA) of the late 1960s (Dickson et al. 1988) when increased Arctic Ocean and ice export (Hakkinen 1993; Serreze et al. 1992) freshened the North Atlantic and reduced deep-water formation in the Labrador Sea (Lazier 1980). Other GSAs have also been documented, some of which have contributions from increased Arctic outflow through the CAA (Belkin et al. 1998). Modeling studies have simulated an influence of Arctic freshwater transport anomalies on the THC (e.g., Delworth et al. 1997; Mauritzen and Hakkinen 1997; Hakkinen 1993; Holland et al. 2001; Mysak et al. 2005) and numerous studies (e.g., Clark et al. 2002; Manabe and Stouffer 1999; Weaver et al. 1999) have suggested that changes in the THC can have far-reaching climatic consequences.

Observations indicate that the Arctic is undergoing considerable and coordinated changes in many different components (e.g., Serreze et al. 2000; Overland et al. 2004). The hydrological cycle at high latitudes and the Arctic Ocean structure and properties are important aspects of this larger observed Arctic climate change. Peterson et al. (2002) document that from 1936 to 1999 the runoff from the six largest Eurasian rivers increased by approximately 7%. Changes in river runoff to the Arctic from North American rivers are more ambiguous, although there is a detectable decrease in river discharge into the Hudson Bay and James Bay (e.g., Dery et al. 2005).

Significant changes in water mass structure and properties within the Arctic Ocean are also evident (e.g., Carmack et al. 1995; Morison et al. 1998; Steele and Boyd 1998). For instance, the Atlantic layer, at 200–800-m depth, has warmed in recent years (e.g., Quadfasel et al. 1991; Polyakov et al. 2004). The cold halocline layer that provides a buffer between the Atlantic layer and the sea ice retreated from 1991 to 1998 although it made a partial recovery from 1998 to 2000 (Boyd et al. 2002). An analysis of data from 1948 to 1993 reveals that much of the upper Arctic Ocean became saltier beginning in 1976, although long time series records are lacking in many regions (Swift et al. 2005). Considerable freshening in some shelf regions also occurred over this time period (Steele and Ermold 2004). Some of these changes are likely related to variability in atmospheric circulation and temperature associated with the Arctic/North Atlantic Oscillation (e.g., Grotefendt et al. 1998; Dickson et al. 2000; Zhang and Hunke 2001). This atmospheric variability can modify sea ice transport and the Fram Strait ice flux (Slonosky et al. 1997; Mysak and Venegas 1998; Kwok and Rothrock 1999; Rigor et al. 2002;), although the relation to Fram Strait ice flux may not be robust on long time scales (Hilmer and Jung 2000). Changes in atmospheric circulation can also modify the Arctic Ocean freshwater exchange to lower latitudes. For example, wind-driven cyclonic/anticyclonic Arctic Ocean circulation regimes have been identified (Proshutinsky and Johnson 1997) that modify the accumulation and release of freshwater within the Arctic (Proshutinsky et al. 2002).

Direct observations of the oceanic flux terms and precipitation over the Arctic Ocean are sparse, making it difficult to assess trends and variability in the Arctic hydrologic system. For example, we still have no complete picture of fluxes through the CAA (Melling 2000). Prinsenberg and Hamilton (2005) cite a volume flux of 0.75 Sv (1 Sv $\equiv 10^6$ m^3 s^{-1}) through Lancaster Sound, but this is only one of the key channels of the CAA. Additionally, the large natural variability present in the Arctic complicates the diagnoses of anthropogenically forced trends in the Arctic climate. As such, coupled climate models are useful in that they provide a complete self-consistent dataset for analysis. Projections into the future can be examined and multiple ensembles can be used to isolate the forced versus naturally varying climate response. While these models still have notable biases, they have improved considerably in their depiction of the Arctic climate. This is in part due to improvements in high-latitude model physics, including the use of more realistic sea ice rheology and subgrid-scale thickness parameterizations, and in part due to improvements in model resolution. This makes them a useful tool for examining Arctic climate change and the processes that contribute to this change.

Several previous studies have examined Arctic freshwater budgets in model simulations. Steele et al. (1996) used a simple ice–ocean model to examine the Arctic Ocean freshwater budget from 1979 to 1985. Their results suggest that variability in the flow through the CAA is quite important and may be out of phase with freshwater export through Fram Strait. Mysak et al. (2005) investigated recent variability in some aspects of the Arctic freshwater budgets using a model of intermediate complexity and found that the model quite accurately simulated ice export variations. Cattle and

Cresswell (2000) diagnosed the mean freshwater budget in a control (present-day) simulation of a coupled climate model. They found that model deficiencies, including no throughflow in the CAA and only simple free-drift sea ice dynamics, led to some important biases in the simulated freshwater transports. Miller and Russell (2000) examined Arctic freshwater budgets in a single climate change integration and found that the model simulated increases in river runoff and net precipitation and decreases in Arctic ice export in response to rising greenhouse gas levels. Numerous additional studies (e.g., ACIA 2005; Wu et al. 2005; Kattsov and Walsh 2000) have used climate models to examine changes in individual terms in the Arctic Ocean freshwater budgets, most notably changes in precipitation and river runoff.

Here we build on these previous studies by examining simulated trends in the Arctic hydrological cycle over the twentieth and twenty-first centuries and their influence on conditions within the North Atlantic. In contrast to previous studies, we use an ensemble of model integrations from simulations being used for the Intergovernmental Panel on Climate Change Fourth Assessment Report (IPCC AR4). In particular, we analyze simulations from the Community Climate System Model version 3 (CCSM3). These integrations and a brief model description are given in section 2. The freshwater budgets over the integration are discussed in section 3. In section 4 we examine the influence of changes in these budgets on the GIN and Labrador Seas and discuss the implications for deep-water formation in these regions. Finally a discussion and conclusions follow in section 5.

2. Model description and simulations

a. Model description

The CCSM3 is a fully coupled, state-of-the-art general circulation model with no flux adjustments. Collins et al. (2006a) give an overall description of the model and its mean climate. Other papers in a special issue of the *Journal of Climate* (Vol. 19, No. 11) describe the model physics and numerous aspects of the climate simulations.

The atmospheric component of the CCSM3 is the Community Atmosphere Model version 3 (CAM3), which uses a T85 (approximately 1.4°) model resolution and 26 levels in the vertical. This model is described by Collins et al. (2006b). The ocean model (Danabasoglu et al. 2006) is a level-coordinate model that is based on the Parallel Ocean Program (POP) model (Smith and Gent 2004). It uses the K-profile parameterization of vertical mixing based on Large et al. (1994) and an isopycnal transport parameterization based on Gent and McWilliams (1990). The model employs a nominally 1° resolution, rotated orthogonal grid in which the North Pole is smoothly displaced into Greenland. This allows for an open Bering Strait and the inclusion of a single open channel through the Canadian Arctic Archipelago. Nares Strait is closed in the model. The sea ice component of CCSM3 is the Community Sea Ice Model (CSIM) (Briegleb et al. 2004; Holland et al. 2006). CSIM uses an elastic–viscous–plastic rheology (Hunke and Dukowicz 1997), energy-conserving thermodynamics (Bitz and Lipscomb 1999), and a subgrid-scale ice thickness distribution (Thorndike et al. 1975; Bitz et al. 2001; Lipscomb 2001). It is run on the same grid as the ocean model. The Community Land Model (CLM3; Dickinson et al. 2006; Bonan et al. 2002) uses a subgrid mosaic of land cover types and plant functional types derived from satellite observations, a 10-layer soil model that explicitly treats liquid water and ice, a multilayer snowpack model, and a river routing scheme. CLM3 is run on the same grid as the atmosphere, except for the river transport scheme, which uses a 0.5° grid.

b. Model simulations

For this study, three different series of model runs are examined. A single, long 1870 control integration was performed to allow the simulated climate to approach equilibrium conditions, although there are still drifts in the deeper ocean. This was run for over 900 yr and is used in this study to provide a characterization of preindustrial conditions. This simulation has constant levels of greenhouse gases, solar input, and other external forcings and as such any long-time-scale trends can be generally attributed to intrinsic model drift and not a response to changes in external forcing. This 1870 integration is used here to diagnose changes in the climate and to evaluate the intrinsic model drift that may contaminate the time series from the twentieth- and twenty-first-century runs. The 1870 run provides the initial conditions for the twentieth-century simulations. It was continued for approximately 500 yr after the twentieth-century integrations were initialized, allowing us to diagnose the intrinsic model drift from these initial conditions.

Simulations from 1870 to 1999 were branched from the 1870 control simulation after it had run for approximately 350 yr of integration. These will be referred to as twentieth-century runs, and they include variations in "external forcings" including sulfates, solar input, volcanoes, ozone, a number of greenhouse gases, halocarbons, and black carbon that are based on the observed

record. A further discussion of the forcing and general climate of these simulations is available in Meehl et al. (2006). An eight-member ensemble of the twentieth-century runs is examined. They differ only in their initial conditions in that they were branched from the 1870 control run at different years. Thus the initial state for the different twentieth-century ensemble runs vary within the simulated natural variability of the 1870 control integration.

Finally, a six-member ensemble of twenty-first-century simulations (from 2000 to 2099) is examined. These runs are continuations of the twentieth-century integrations with each ensemble member starting from a different twentieth-century ensemble run. The simulations use the IPCC Special Report on Emissions Scenarios (SRES) A1B scenario (Houghton et al. 2001) of external forcing. This scenario assumes rapid economic growth, a global population that peaks midcentury and declines thereafter, the rapid introduction of new and more efficient technologies, and a balance across fossil and nonfossil fuel sources. As the details of the forcing scenario will influence the time series evolution and can modify our conclusions, we have also examined single integrations from the SRES A2 and SRES B1 scenarios. These scenarios have been used in the IPCC assessment reports and represent relatively high (A2) and low (B1) emissions of greenhouse gases compared to the SRES A1B scenario. While we focus here on the ensemble results from the SRES A1B integrations, the comparison to these other future scenarios allows us to address some of the uncertainties that arise from the choice of future emission scenario. A further discussion of these simulations and their general climate is given in Meehl et al. (2006).

c. *Model performance in the Arctic*

The simulated ensemble mean ice thickness from 1980 to 1999 for March and September is shown in Fig. 1. The 15% contour interval of ice concentration from both the model ensemble and the Special Sensor Microwave Imager (SSM/I) observations (Cavalieri et al. 1997) is also shown. The model simulation of ice extent is quite reasonable. However, as indicated in Fig. 1 and confirmed by the annual cycle of ice extent (Fig. 2), the simulated winter ice cover is from 1 to 1.8 million km^2 more extensive than observed from January through May. This is associated with excessive ice extent in the Labrador Sea and North Pacific. The Barents Sea has too little ice cover compared to observations, which is related to an anomalously warm Atlantic inflow to the Arctic. In contrast to the winter conditions, from June to December, the observed and simulated Northern Hemisphere ice extents are in excellent agreement and the differences between the two are generally smaller than the standard deviation associated with interannual variability over the 20-yr climatology shown in Fig. 2.

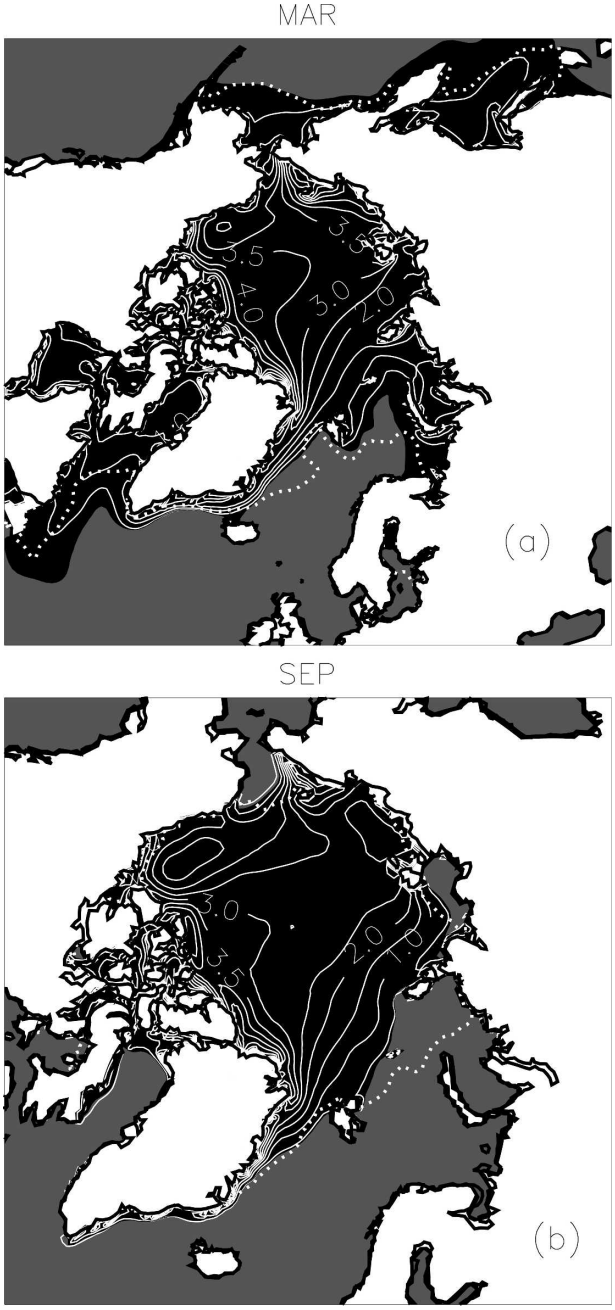

FIG. 1. The simulated ensemble mean ice thickness averaged from 1980 to 1999 for (a) March and (b) September. The contour interval is 0.5 m. The black region indicates the simulated ice that has higher than 15% ice concentration on the annual average. The annual average 15% ice concentration contour from satellite observations is shown by the dotted line.

Observations of ice thickness are based on sparse

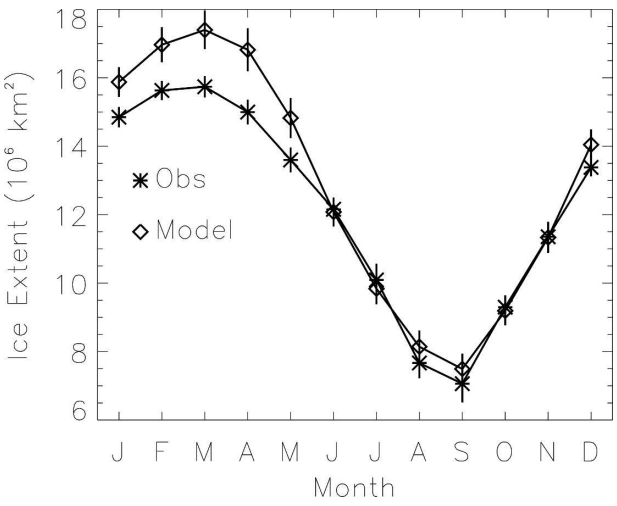

FIG. 2. The annual cycle of Northern Hemisphere ice extent from the simulated climatological ensemble mean from years 1980 to 1999 and from the satellite SSM/I observations.

submarine observations (e.g., Bourke and Garrett 1987) or more recently on satellite altimetry data (Laxon et al. 2003), which have no coverage at latitudes greater than 81.5°N or in the marginal ice zone. Consistent with observations, the model shows the thickest ice along the Canadian Arctic Archipelago and north of Greenland, although the ice in the East Siberian Sea is overly thick. This simulated ice thickness pattern is a considerable improvement compared to older model versions (e.g., Weatherly et al. 1998) and is partly associated with changes in atmospheric resolution and wind forcing of the sea ice as discussed by DeWeaver and Bitz (2006). For comparison to the satellite altimetry data, we have computed the mean October–March thickness, excluding thin ice (less than 1 m), for the region south of 81.5°N. The simulated value of 2.6 m compares quite well to the value of 2.73 m obtained by Laxon et al. (2003) from satellite altimetry measurements.

The sea surface salinity (SSS) from the model and the Polar Hydrographic Climatology (PHC) observations (Steele et al. 2001) are shown in Fig. 3. The model reproduces the fresh shelf conditions present in the observations although it is perhaps too fresh in these areas. Additionally, the simulated central Arctic is too saline compared to observations, which suggests that the shelf waters remain too confined along the coasts. However, considerable trends are observed in the shelf waters and the transport of these waters into the deep ocean (Steele and Ermold 2004), which may affect this comparison. Because of biases upstream in the North Atlantic, the inflow in the Barents Sea is anomalously saline, which may contribute to the high salinity within the central Arctic.

The vertical profiles of annual average temperature and salinity averaged from 80° to 90°N are shown compared to the PHC data in Fig. 4. The model is biased fresh and cold in the upper 40 m. Below this the simulated temperatures are too warm, which is associated with biases in the temperature of the Atlantic layer inflow to the Arctic. These result from errors in the Gulf Stream path within the North Atlantic. Deeper than approximately 200 m, the simulated ocean is relatively saline compared to the observed climatology. The model simulates a strong halocline, as seen in observations. There is also some evidence in the simulations of a cold halocline layer as the increasing salinities occur higher in the water column than the increasing temperatures. However, this is very weak compared to the observations. The presence of the CHL may have important implications for ice–ocean heat exchange (Aagaard et al. 1981; Steele and Boyd 1998).

Aspects of the Arctic atmospheric conditions from a control simulation of the CCSM3 are discussed by DeWeaver and Bitz (2006). In general, the Arctic sea level pressure (SLP) is too low and the Beaufort high is too weak. The surface winds associated with this lead to biases in the sea ice transport. The simulated ice velocity field (Fig. 5a) does exhibit a Beaufort gyre and Transpolar Drift Stream as in observations (Fig. 5b). However, the Beaufort gyre is displaced poleward from its observed location. As discussed below, the mean ice export through Fram Strait is reasonably simulated. There are also biases in the polar radiation fluxes and cloud cover in this model, as discussed in Collins et al. (2006a). Most notably, this includes a considerable deficit in the downwelling shortwave radiation at the surface as compared to observations (e.g., Persson et al. 2002).

3. Simulated Arctic Ocean freshwater budgets

Although the simulated Arctic has some notable biases as discussed above, the model reasonably captures many of the large-scale features of the observed high-latitude climate system. This suggests that the model can provide valuable information on trends and variability within the climate and give insight into the processes that drive this variability. This has been born out by previous studies (e.g., Holland 2003; Goosse and Holland 2005) that investigated Arctic climate variability in an earlier incarnation of this model. Indications are that these earlier results are relevant to the current model diagnosed here, which has nearly identical sea ice and ocean components. Here we focus on the Arctic

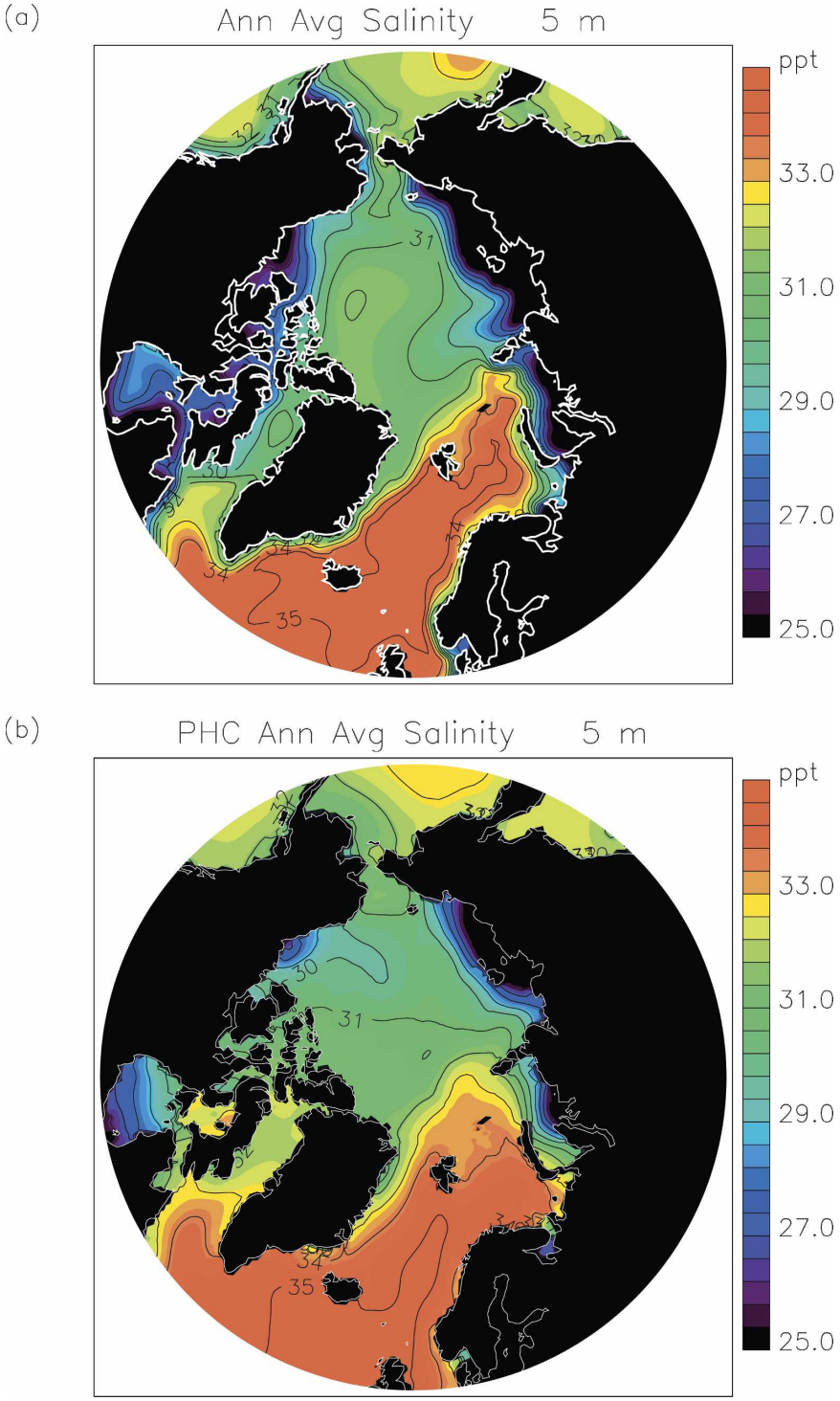

FIG. 3. The annual averaged sea surface salinity from (a) the ensemble mean model simulation and (b) the PHC (Steele et al. 2001). The model output represents the mean conditions from 1980 to 1999. The line contour interval is 1 ppt.

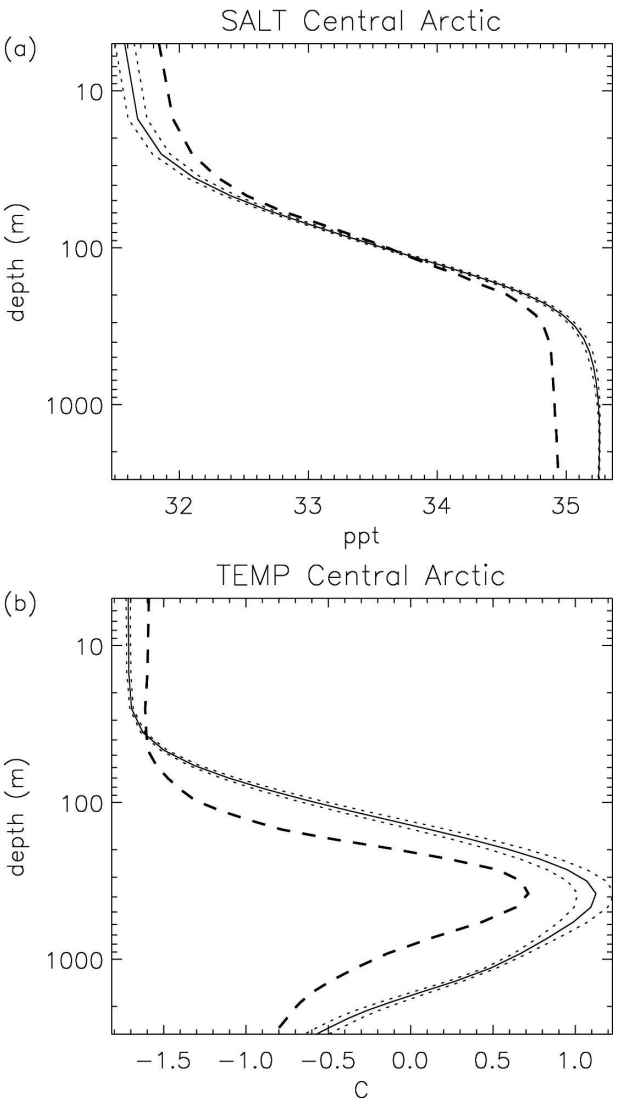

FIG. 4. The annual average (a) salinity and (b) temperature profile averaged from 80° to 90°N for the ensemble mean model simulation (solid line) and the PHC climatology (dashed line). The model data were averaged from years 1980 to 1999. The dotted line shows the spread for the different ensemble members.

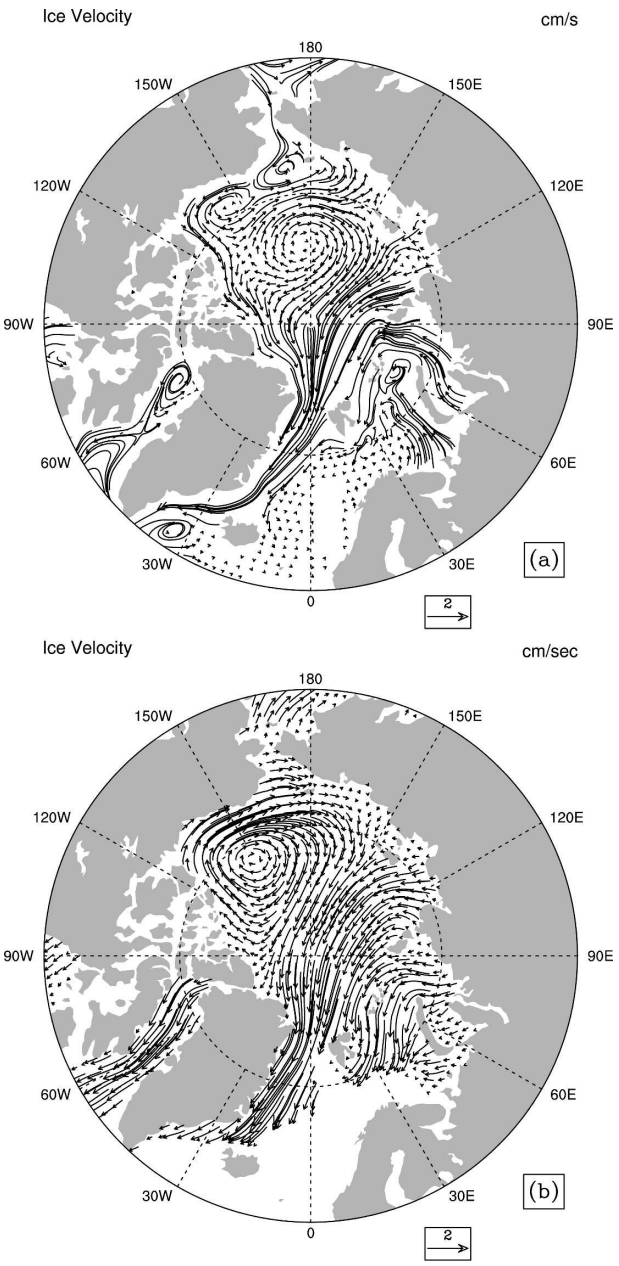

FIG. 5. The 1980–99 averaged ice velocity in cm s^{-1} for the (a) ensemble model average and (b) satellite observations (Fowler 2003). The vectors are represented using a curved polyline tangent to the instantaneous flow in the neighborhood of the grid point.

freshwater budgets in the twentieth and twenty-first centuries. Trends in these budgets, the mechanisms driving these trends, and potential implications for ocean deep-water formation in the North Atlantic are specifically addressed.

For the purposes of this study, the Arctic basin is defined as the ocean area enclosed by a number of transects across ocean straits (Fig. 6). These transects include Fram Strait, a section across the Barents Sea, the Bering Strait, and a transect across the CAA, specifically across M'Clure Strait. The CAA contains only a single direct channel between the Arctic and Baffin Bay—with Nares Strait being closed on the model grid because of limited model resolution. This is an important shortcoming of the model and, as discussed in section 3a, leads to low simulated transports in this region. The freshwater transport, M, is computed as

$$M(u, S) = L \int_{-230\text{m}}^{0} u \frac{(S_0 - S)}{S_0} dz, \qquad (1)$$

FIG. 6. The regions and transects used in the model analysis. The Arctic Ocean domain is bounded by transects (shown in red) across Fram Strait, the Barents Sea, Bering Strait, and M'Clure Strait (in the Canadian Arctic Archipelago). The GIN Seas and Labrador Sea/Baffin Bay regions used in the analysis are indicated by the dashed lines.

where L is the length of the transect, $\mathbf{u}$ is the velocity perpendicular to the transect, S is the salinity, and S_0 is a reference salinity. We use a reference salinity of 34.8 psu following Aagaard and Carmack (1989) and Steele et al. (1996) to compute the ocean and sea ice freshwater transports. This allows for a more direct comparison to previous studies. Additionally, for consistency with Steele et al. (1996) we compute the ocean transport terms over the upper 230 m of the water column. This makes essentially no difference for the transport through the CAA, the Bering Strait, or across the Barents Sea transect because these are regions whose depths are generally shallower than 230 m. For the Fram Strait throughflow the freshwater transport is approximately 14% lower when computed over the full depth, but the trends and variability are nearly identical, suggesting that the upper water column is most important in driving these trends.

a. Mean budgets

The mean values and standard deviations of terms that contribute to the Arctic Ocean freshwater budget averaged over the twentieth century are shown in Table 1 along with observed values. At the large scale, and in agreement with observations, the rivers and net precipitation freshen the Arctic Ocean while the ocean and ice exports remove this freshwater from the basin. The rivers and net precipitation compare reasonably well to

TABLE 1. Twentieth-century average Arctic Ocean freshwater budget in Sv for the model simulations. Observed climatological estimates from various sources are shown for comparison.

Term	Mean	Std dev	Observed value	Reference for observed value
Ocean transport				
Total	−0.090	0.026		
Fram Strait	−0.149	0.019	−0.100 −0.031	Meredith et al. 2001; D06; Aagaard and Carmack 1989
CAA	−0.053	0.007	−0.099 −0.029	Prinsenberg and Hamilton 2005; Kleim and Greenberg 2003; Aagaard and Carmack 1989
Barents Sea	0.016	0.011	−0.002 −0.009	Blindheim 1989; D06; Aagaard and Carmack 1989
Bering Strait	0.097	0.014	0.076 0.053	Woodgate and Aagaard 2005; Aagaard and Carmack 1989
Ice transport				
Total	−0.104	0.027		
Fram Strait	−0.106	0.025	−0.075 −0.057	Vinje 2001; Kwok et al. 2004
Barents Sea	−0.004	0.005	−0.001	Kwok et al. 2005
Bering Strait	0.005	0.003	0.003	Woodgate and Aagaard 2005
River runoff				
Total	0.115	0.0065	0.094	Lammers et al. 2001
Eurasian	0.096	0.0062	0.071	Lammers et al. 2001
North America	0.019	0.0015	0.023	Lammers et al. 2001
Atmospheric fluxes				
$P - E$	0.057	0.0043	0.065	S06

observational estimates (e.g., Lammers et al. 2001; Serreze et al. 2006, hereafter S06), especially considering the errors in river discharge data (e.g., Shiklomanov et al. 2006), uncertainties in the ungauged portion of river runoff (Lammers et al. 2001), and the limited precipitation observations over the Arctic Ocean (e.g., Cullather et al. 2000).

The simulated Fram Strait ice export is approximately 40% larger than the Vinje (2001) observations and 80% larger than the Kwok et al. (2004) observations. These observations use only limited information on ice thickness to derive an ice volume flux. Additionally, they are only available for the later part of the twentieth century. When a consistent averaging period is used, the model compares more favorably to these observed estimates but is still approximately 10% larger than the Vinje (2001) data. There is a small ice loss across the Barents Sea transect and a net transport of sea ice into the Arctic Ocean from the Bering Sea. The Bering Strait ice transport agrees quite well with the recent observations of Woodgate and Aagaard (2005).

The net ocean transport includes contributions across the different transects. The Bering Strait freshwater transport (Table 1) freshens the Arctic Ocean, but the values are 28% larger than the observations of Woodgate and Aagaard (2005). The simulated Bering Strait mass transport is quite reasonable, averaging approximately 1 Sv. However, the waters entering the Arctic through the Bering Strait are anomalously fresh, which is related to excessive runoff from the simulated Yukon River.

In contrast to the observations, the simulated Barents Sea transport also provides a small source of freshwater to the Arctic. Although the "Atlantic" core of this water is quite saline, there are fresh contributions from river runoff into the Barents Sea and from the relatively fresh Norwegian Coastal Current that penetrate into the Arctic along the coast of Novaya Zemlya. There are indications that the river runoff into the Barents Sea is too large, which may account for some of the bias in the simulated Barents Sea freshwater transport when compared to observed estimates (Table 1). Observations (Blindheim 1989) suggest that the Norwegian Coastal Current provides a freshwater import of approximately 0.008 Sv to the Arctic Ocean. Estimates of the Atlantic freshwater inflow to the Barents Sea range from −0.017 (Aagaard and Carmack 1989) to −0.01 Sv (Dickson et al. 2006, hereafter D06), resulting in a total freshwater import to this region of between −0.009 and −0.002 Sv depending on the observations.

The ocean transports through Fram Strait and the CAA are both sinks of freshwater for the Arctic basin as relatively fresh Arctic waters are transported into the North Atlantic. There are numerous and varied observational estimates of these transports in the literature. Recent estimates from Prinsenberg and Hamilton (2005) based on 3 yr of observations indicate a mean

freshwater transport of 0.046 Sv through Lancaster Sound. This agrees very well with our simulated value. However, modeling studies (Kleim and Greenberg 2003) suggest that the transport through Lancaster Sound makes up only 40%–50% of the fluxes through the CAA. Thus, it appears that the poor resolution of the narrow channels within the CAA of the model (and thus the absence of a Nares Strait, e.g.) contributes to an underestimate of the total freshwater transport through this region into Baffin Bay.

The simulated liquid freshwater export across Fram Strait represents a 0.149 Sv loss of freshwater for the Arctic Ocean. This includes contributions from the EGC outflow of fresh Arctic waters and the West Spitsbergen Current (WSC) inflow of relatively saline Atlantic waters. Observations suggest an average EGC meteoric water flux of 0.09 Sv for 1997–98 with a large (0.054 Sv) difference between the two years (Meredith et al. 2001). The freshwater flux is approximately half that of the meteoric water flux (which does not account for sea ice contributions; Meredith et al. 2001; Bauch et al. 1995). This results in an approximate EGC average freshwater export of 0.045 Sv for these two years. The WSC contribution to the Fram Strait flux is quite uncertain, with observed values ranging from 0.005 (Aagaard and Carmack 1989) to 0.024 Sv (D06). Even using the largest values cited for the observed EGC and WSC transports, the simulated Fram Strait freshwater export is about 50% larger than the observed estimate. However, there are considerable uncertainties in the transport estimates for this region (e.g., Carmack 1990).

The ice and ocean transports have considerable interannual variability, as indicated by the large standard deviations shown in Table 1. In the case of Fram Strait ice export, where relatively long observed time series exist, the simulated standard deviation compares very well to the observed value of 0.021 Sv (Vinje 2001). Variations in the river runoff and net precipitation are reasonable compared to observed estimates (S06) and are considerably smaller than the ocean flux terms.

b. Trends

The time series of the large-scale components of the Arctic Ocean freshwater budget over the twentieth and twenty-first centuries are shown in Fig. 7. The sign convention is such that a source of freshwater for the Arctic Ocean is positive and a sink is negative. Results from the 1870 preindustrial control integration are also shown on this figure. These provided the initial conditions for the twentieth-century integrations. While there is considerable interannual variability in the preindustrial control integrations, the results shown in Fig. 7 indicate that there is relatively small intrinsic model drift in these terms.

1) River runoff

An increasing trend is present in the ensemble average river runoff (Fig. 7a) over the twentieth and twenty-first centuries. This trend is largely due to increases in the Eurasian runoff, with North American rivers contributing a smaller amount. This is not surprising since most of the river runoff into the Arctic come from Eurasia. The Eurasian contribution to the total Arctic runoff is relatively stable over the integration, decreasing slightly from 83% to 82% of the total runoff over the twenty-first century. Over the twentieth century, the simulated change amounts to a 7% increase in the Eurasian runoff. This is in excellent agreement with the changes observed by Peterson et al. (2002) from 1936 to 1999. The twentieth-century ensemble mean trend is significantly different from zero at the 95% level. However, twentieth-century trends within the individual ensemble members are not significant for all of the members because of the large internal variability in the time series. The trend in river runoff accelerates into the future, with the maximum 50-yr running trend (Fig. 8) occurring from year 2000 to year 2050. This is consistent with the trends in the fall and winter terrestrial precipitation, which are at a maximum from 2000 to 2050. By the end of the twenty-first century, a further 20% increase in runoff occurs compared to the 2000 conditions. The twenty-first-century trends for both the ensemble mean and individual ensemble members are significant at the 95% level.

Arctic river discharge is an aggregate measure of the water balance over the extensive Arctic drainage basin and is influenced by changes in precipitation (P), evapotranspiration (E), and terrestrial water storage (S). Examining these terms for the watersheds that feed the Arctic Ocean reveals that the increase in Arctic discharge in the twenty-first-century ensemble members is due to a weak, positive trend in total annual net precipitation ($P - E$) over the Arctic drainage basin. Although yearly totals of both P and E increase as mean surface air temperatures rise, trends in P are typically larger than those in E, leading to increased delivery of moisture to the land surface.

This agrees well with recent observations (Peterson et al. 2002; Grabs et al. 2000; Serreze et al. 2003) and other modeling studies (e.g., Arora and Boer 2001). Concurrent negative trends in average soil moisture indicate that none of the additional $P - E$ remains in the soil, and must all be contributing to increased discharge. The decrease in soil moisture is considerably

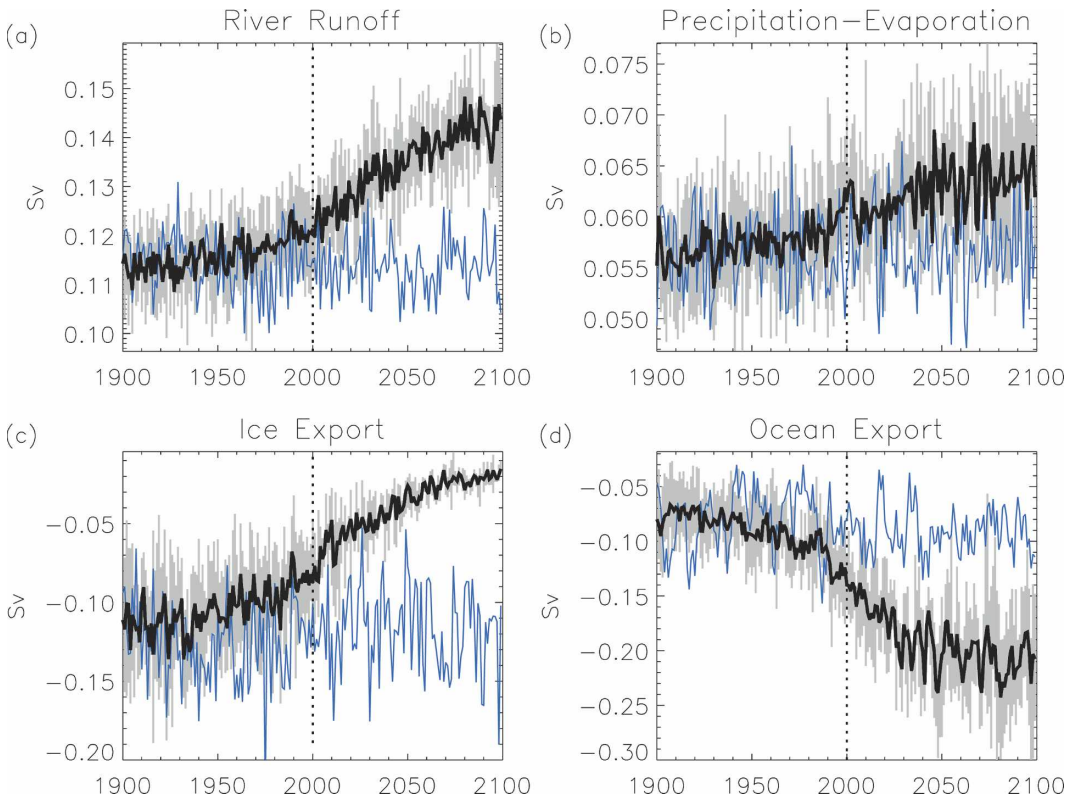

FIG. 7. The time series of (a) river runoff, (b) net precipitation, (c) sea ice export, and (d) ocean export in Sverdrups of freshwater over the twentieth and twenty-first centuries. The sign convention is such that a source of freshwater for the Arctic Ocean is a positive value. The ensemble mean is shown by the black line, and the gray envelope about the mean indicates the range in the individual ensemble members. The thin blue line shows results from a preindustrial (1870) control integration from years 450–650. These provided the initial conditions for the twentieth-century integrations, with different twentieth-century ensemble members starting from different years of the 1870 run.

less than the increase in $P - E$ and contributes little to rising discharge. These trends were found in all but the Ob basin, where changes in annual P and E were roughly balanced, leaving no significant trend in $P - E$. The simulated Ob basin has considerably higher summer soil moisture than other regions in the Eurasian drainage basin, allowing for larger increases in evaporation.

The character of these changes is further revealed by a consideration of individual seasons. Consistent with observations (e.g., Serreze et al. 2003), both P and E have a summer maximum over the Arctic watersheds resulting in small (in some locations even negative) net summer precipitation. Over most of the regions considered, P shows similar increasing trends in all seasons, though in the Ob and Yenisei basins the weakest trends occur during the summer. In contrast, E increases little during the winter, autumn, and spring but shows a pronounced rise during the summer. This leads to an increase in the net precipitation in the winter, spring, and fall (and in the annual average). Because the summer E increase is nearly equal to or sometimes exceeds the summer P increase over the majority of the Eurasian portion of the Arctic drainage basin, weak negative summer $P - E$ trends often result. Although these negative trends are not statistically significant, they do suggest that decreased soil moisture is largely the result of summer drying. This is consistent with several observational studies (Grabs et al. 2000; Serreze et al. 2003).

2) NET PRECIPITATION

Net precipitation over the Arctic Ocean (Fig. 7b) also increases over the twentieth and twenty-first centuries. Similar to the river runoff, this trend is associated with increases in both precipitation and evaporation, with the increased precipitation winning out on the annual average. The ensemble mean trend is significant. However, for some individual ensemble members, no significant trend is present over either the

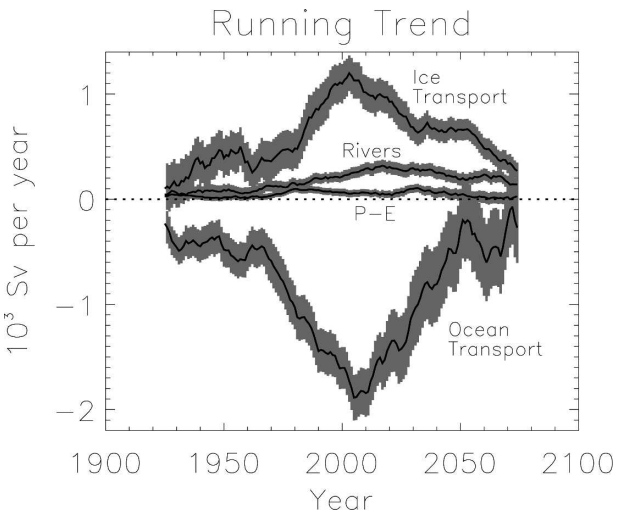

FIG. 8. The 50-yr running trend for the major components of the Arctic Ocean freshwater budget, including the total ocean transport, the total ice transport, the river runoff, and the net precipitation ($P - E$) over the twentieth and twenty-first centuries. The sign convention is such that a source of freshwater for the Arctic is a positive value, so a positive trend indicates an increasing source (or decreasing sink) of freshwater for the Arctic Ocean. The 95% confidence intervals are indicated by the dark shading. The values are plotted relative to the middle year used in the trend analysis, so the values for 1925 show the trend for 1900–50.

twentieth or twenty-first-century time series. This indicates the difficulty in detecting such trends from the observational time series, which only has a single realization that is subject to large natural variations. From the ensemble mean time series, there is a 6% increase in the net precipitation over the twentieth century and a further 8% increase by 2100.

3) SEA ICE TRANSPORT

Sea ice export, which is a sink of freshwater for the Arctic Ocean and hence denoted by negative values in Fig. 7c, significantly decreases over the twentieth and twenty-first centuries. Over the twentieth century, the ice freshwater flux decreases by 0.03 Sv or 28%. This is largely due to changes near the end of the century when the ice has started to thin considerably. This thinning is consistent with observations and hindcast simulations using stand-alone ice–ocean coupled models (e.g., Rothrock et al. 1999, 2003; Rothrock and Zhang 2005). The maximum 50-yr running trend in the ice transport (Fig. 8) is obtained from approximately 1975 to 2025, which is associated with a large decrease in the net ice growth rates and a thinning ice cover.

The trends continue into the future and level off near the end of the twenty-first century, at which time the ice export has undergone a 76% decrease compared to the year 2000. The interannual variability in ice export as exhibited by the envelope about the ensemble mean has also decreased considerably in the twenty-first century, indicating that in a warmer climate, variations in sea ice export may be less important for driving climate variability. This is consistent with results from an intermediate complexity model that showed decreased sea ice induced thermohaline circulation variability in a warmer climate (Holland et al. 2000). The decrease in ice export over the twentieth and twenty-first centuries represents a decrease in net Arctic ice growth (which equals the total annual ice growth minus the total ice melt) and increased freshening for the Arctic Ocean.

The decreased annual average net ice growth results largely from increases in summer melting. Until approximately 2040, this is partially compensated by increases in the annual average ice growth as a thinning and less insulating ice cover allows for increased cold season ice production. As discussed by Bitz et al. (2006), increased fall/winter ice growth and brine rejection under a warming climate can have important consequences for ocean circulation and heat transport to the Arctic basin. After approximately 2040, the warming at high latitudes overwhelms the reduced ice insulating effect, and the annual average Arctic ice growth decreases.

4) OCEAN TRANSPORT

Trends in rivers, net precipitation, and sea ice processes over the twentieth and twenty-first centuries all contribute to a freshening of the Arctic Ocean. This increases the storage of freshwater in the Arctic Ocean (Fig. 9), resulting in fresher waters being exported from the Arctic through Fram Strait and the CAA. This contributes to changes in the Arctic Ocean freshwater export (Fig. 7d), which exhibits a significant increase of 65% over the twentieth century and a further 87% over the twenty-first century. Similar to the ice transports, the 50-yr running ocean transport trend (Fig. 8) is largest from approximately 1975 to 2025. This is related to the large net ice melt and consequent ocean freshening over this time period.

The ocean freshwater transport time series through the various straits that define the Arctic Ocean domain are shown in Fig. 10. Increased freshwater export through the Fram Strait and, to a lesser extent, the CAA are responsible for the twentieth–twenty-first-century trend in total ocean transport. It is worth noting that the limited resolution of the CAA will affect these projections. The increased freshwater loss to the North Atlantic is compensated by small increases in freshwater import through the Bering Strait in the twentieth

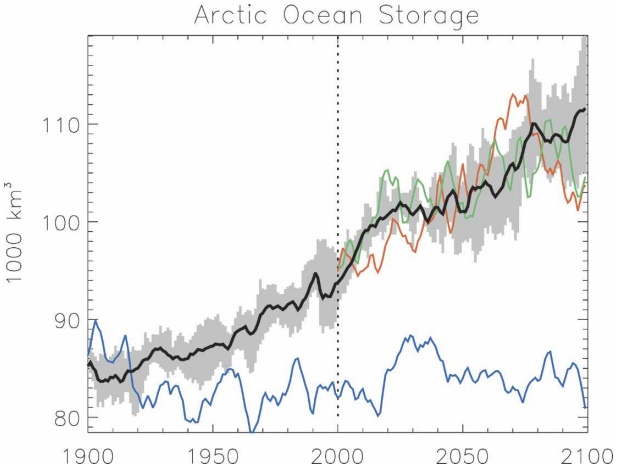

FIG. 9. The time series of liquid freshwater stored in the Arctic Ocean over the twentieth and twenty-first centuries. The ensemble mean value is shown by the black line, and the gray envelope indicates the range in the individual ensemble members. The green and red lines indicate the time series from single integrations using the SRES A2 and B1 scenarios, respectively. The thin blue line shows the values from the preindustrial control integration.

century. However, Bering Strait trends are negligible over the twenty-first century. The Barents Sea exchange shows only small changes over the twentieth century. In the twenty-first century, increases in the Barents Sea freshwater import to the Arctic partially compensate for the increased freshwater loss through Fram Strait and the CAA.

As the Arctic Ocean salinity is decreasing, it is not surprising that the oceanic freshwater export from the Arctic to lower latitudes increases. However, changes in ocean circulation may also be important in driving these freshwater transport changes. To assess this, we separately compute the influence of the time-varying salinity (S') and the influence of the time varying velocity (u') on the freshwater transport using $M(\overline{u}, S')$ and $M(u', \overline{S})$, as defined in Eq. (1). For these calculations, the $\overline{u}$ and $\overline{S}$ terms represent the twenty-first-century time-averaged local velocity and salinity, respectively, and the u' and S' terms represent the departure in the local velocity and salinity from these long-term means.

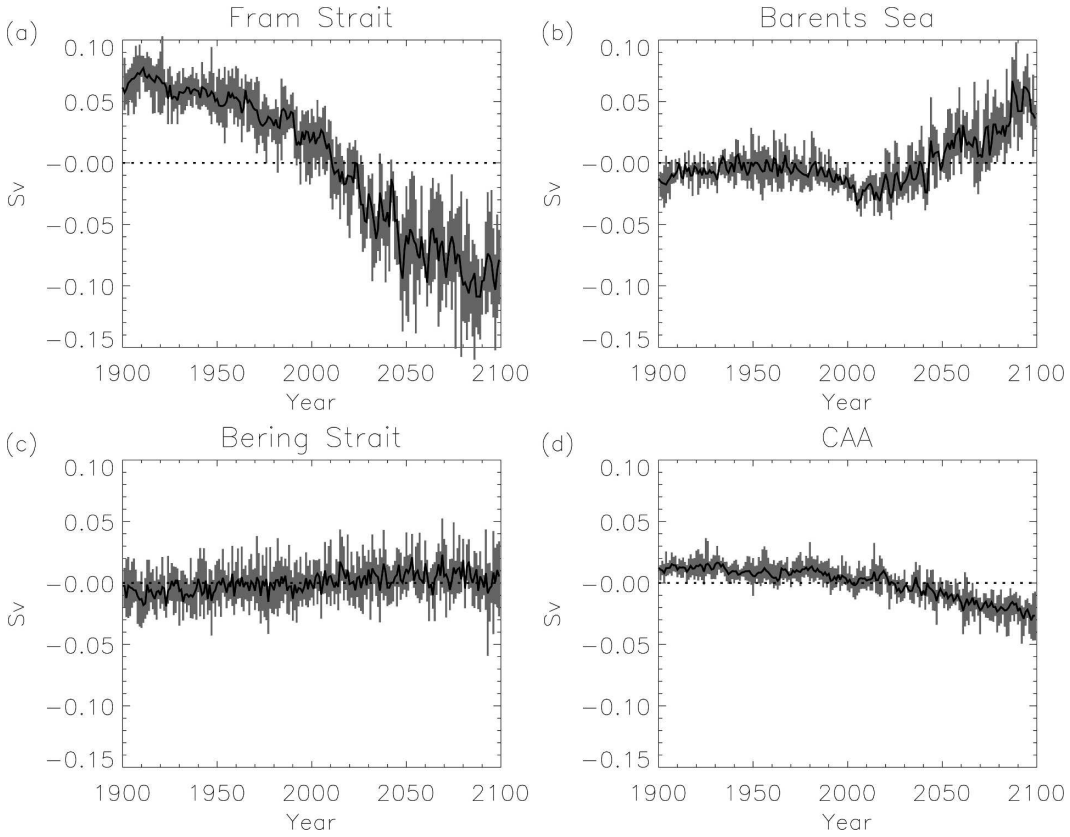

FIG. 10. The twentieth–twenty-first-century time series of the ocean liquid freshwater transport anomalies in Sv for different straits. Shown are transports through (a) Fram Strait, (b) the Barents Sea, (c) Bering Strait, and (d) the CAA.

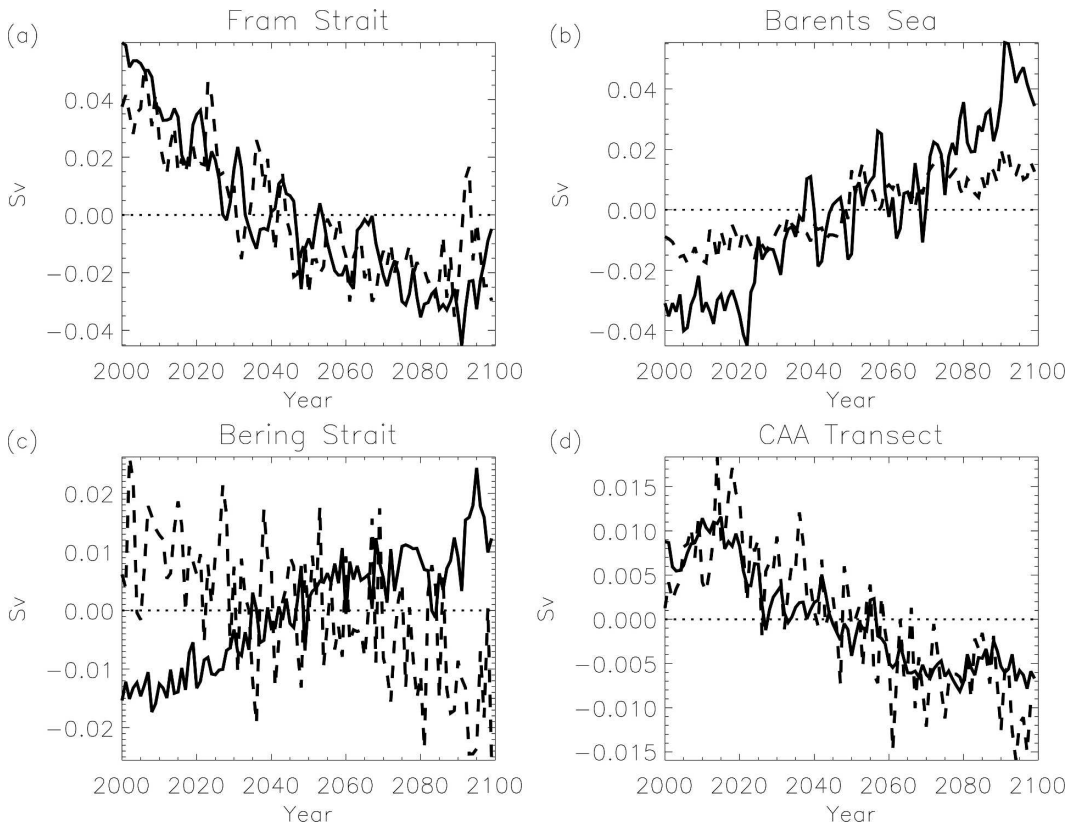

FIG. 11. The ensemble mean time series in Sv of the contribution from variable velocity (dashed line) and variable salinity (solid line) to the anomalous ocean freshwater transport through different straits over the twenty-first century. Shown are the transports through (a) Fram Strait, (b) the Barents Sea, (c) Bering Strait, and (d) the CAA.

Figure 11 shows the anomalous contributions from variable salinity and variable velocity to the oceanic transport over the twenty-first century for different straits. It clearly exhibits that ocean circulation changes are important for the simulated trends. In particular, increased velocities in the East Greenland Current and the CAA, resulting in increased ocean mass transport, are as important as salinity changes for driving the freshwater export trends in these straits. In contrast, while the waters entering the Arctic through the Bering Strait are fresher, there is also less of them (e.g., the mass transport is reduced). This change in ocean circulation is associated with a reduced sea surface height difference, and hence smaller "pressure head," between the Pacific and the Arctic due to relatively large increases in Arctic sea level over the twenty-first century. The reduced velocity and fresher waters compensate in terms of the freshwater transport, resulting in very little change in the Bering Strait contribution to the Arctic Ocean freshwater budgets over the twenty-first century. The increased freshwater import through the Barents Sea is almost entirely driven by changes in the salinity of these waters.

5) UNCERTAINTY IN FUTURE PROJECTIONS ASSOCIATED WITH THE FORCING SCENARIO

There is considerable uncertainty in how emissions of greenhouse gases will change in the future. Here we assess the uncertainty in the simulated future projections that are associated with the forcing scenario by examining two additional simulations that are forced with the SRES A2 and SRES B1 scenarios. Compared to the SRES A1B scenario, these represent relatively high (A2) and low (B1) emissions of greenhouse gases. The initial conditions for all of these twenty-first-century runs were obtained from the same twentieth-century ensemble members.

Figure 12 shows the 50-yr running trend in the freshwater terms from these integrations. For comparison, the trends in the different ensembles of A1B simulations are indicated by the gray shading. The net precipitation trend is not shown on this figure but is gen-

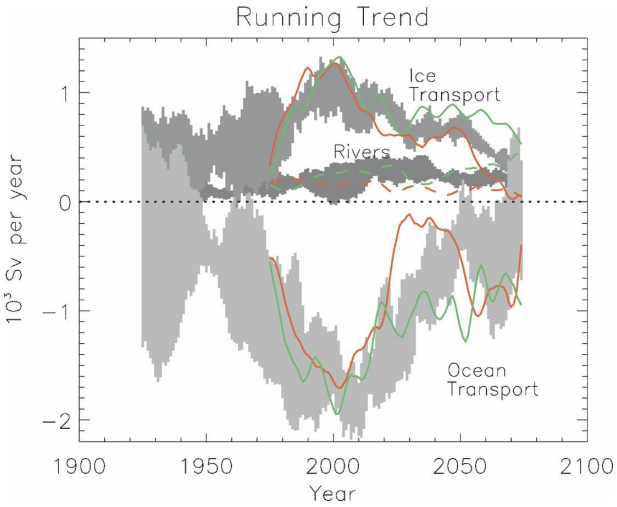

FIG. 12. The 50-yr running trend for the total ocean transport, the total ice transport, and the total river runoff over the twentieth and twenty-first centuries for the SRES A1B ensemble members (gray shading), the A2 scenario (green), and the B1 scenario (red).

erally small for all of the runs. In all integrations, the maximum 50-yr ice and ocean transport trends occur from approximately 1975 to 2025. This is perhaps not surprising since they all have identical twentieth-century integrations and large net ice melt from 1975 to 2000. The timing for the maximum river runoff and P − E trends are more variable among the different forcing scenarios. In general, the B1 integration has the lowest river runoff trends in the twenty-first century with a maximum 50-yr trend from 1957 to 2007. The A2 and A1B scenarios have similar runoff trends over much of the twenty-first century, but the A2 run has generally larger changes in the latter part of the twenty-first century. The timing of the maximum net precipitation trends for the B1 and A2 integrations falls within the timing of the maximum trends for the different A1B ensemble members.

The trends in the large-scale Arctic freshwater budget terms over the twenty-first century for the different scenario integrations are shown in Table 2. The large range in simulated net precipitation trends for the different SRES A1B ensemble members indicates that net precipitation trends over the Arctic Ocean are indistinguishable among the different forcing scenarios. For the other budget terms, the SRES A2 simulation has the largest trends and the SRES B1 simulation has the smallest trends. This is consistent with the relatively high (A2) and low (B1) forcings for these scenarios. Except for the B1 ocean transport, the A2 and B1 trends are outside the range of trends in the different A1B ensemble members. For all scenarios, increasing twenty-first-century Arctic Ocean freshwater export is balanced in part by increasing river runoff and decreasing ice export.

TABLE 2. Trend of freshwater budget terms over the twenty-first century for different scenarios in Sv (100 yr)$^{-1}$. For the A1B scenario the minimum and maximum trends among the different ensemble members are shown.

	Ocean transport	Ice transport	Net precipitation	River runoff
A1B	−0.04/−0.08	0.05/0.06	0.001/0.007	0.02/0.02
A2	−0.09	0.07	0.006	0.03
B1	−0.05	0.04	0.003	0.01

4. Influence of changes in Arctic freshwater budgets on the GIN and Labrador Seas

As indicated by the simulated deep ocean mixed layers (Fig. 13), which are associated with deep-water production, the GIN Seas and Labrador Sea are two important deep-water formation regions in the simulated climate. An additional deep-water formation region occurs along the southern edge of the Greenland–Scotland ridge. Changes in the freshwater exchange between the Arctic and northern North Atlantic can directly modify ocean conditions in these regions and thus may be important for changes in the thermohaline circulation over the twentieth and twenty-first centuries. Because of their relative magnitude, here we focus on changes that occur over the twenty-first century.

a. The GIN Seas

Over the twenty-first century, the GIN Seas receive reduced freshwater transport in the form of Arctic sea ice but increased liquid Arctic freshwater transport. The net result is an increased Arctic freshwater flux into the GIN Seas. This contributes to a decreasing trend in the upper-ocean salinity within the GIN Seas over the first half of the twenty-first century (Fig. 14). However, although the trend in Arctic Ocean freshwater flux to the GIN Seas increases throughout the twenty-first century, the GIN Sea upper-ocean salinity only decreases until approximately 2050. The upper-ocean GIN Sea density does decrease over the twenty-first century, but this is largely a result of warming temperatures, with salinity changes having only a small influence (Fig. 14).

The density changes are clearly not uniform across the GIN Seas, and the contribution to the changing density from changes in temperature and changes in salinity vary across the GIN Seas (Fig. 15). A large

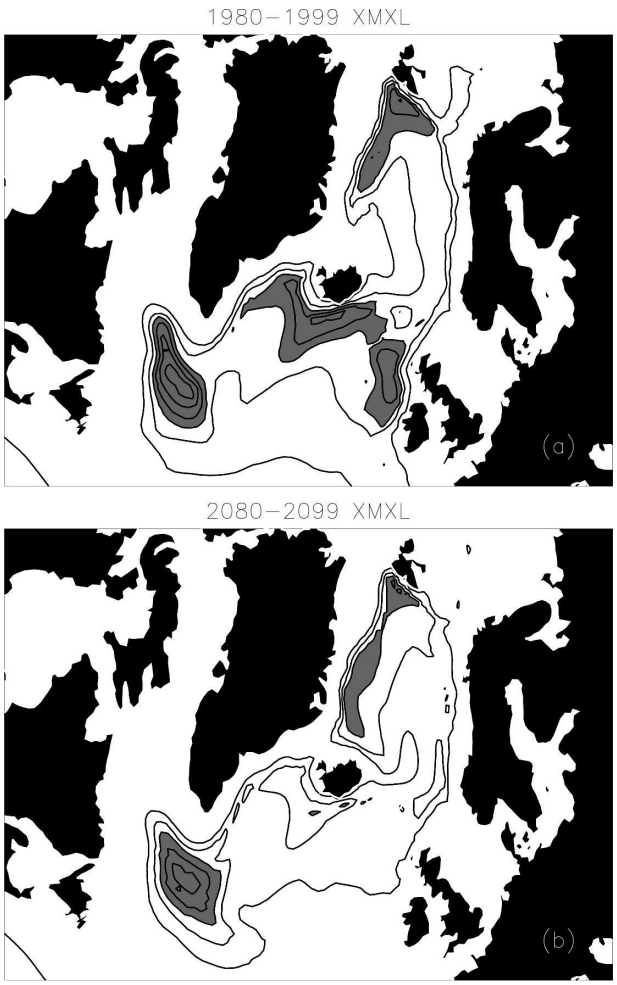

FIG. 13. Maximum climatological ocean mixed layer depths averaged from (a) 1980 to 1999 and (b) 2080 to 2099. The ocean mixed layer is obtained from the maximum vertical buoyancy gradient between the surface and ocean depth as discussed by Large et al. (1997). The maximum value for each month at each grid cell is saved during model run time, and these values are averaged over the 20-yr period to obtain the maximum mixed layers shown here. The contour interval is 100 m, and regions of greater than 300 m are shaded.

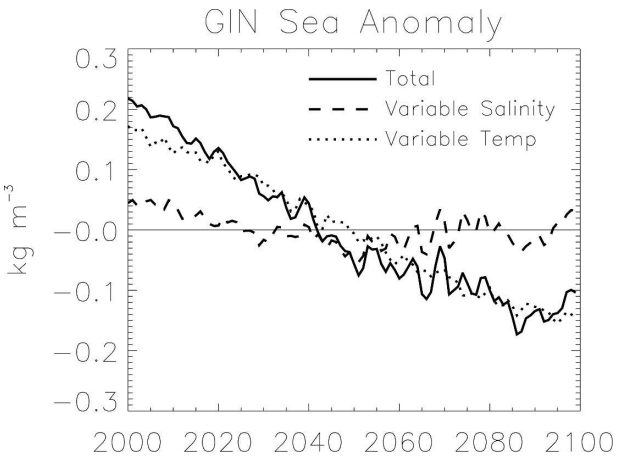

FIG. 14. The twenty-first-century time series of the ensemble mean GIN Sea upper-ocean (0–230 m) average density anomaly in kg m^{-3}. The region used for this analysis is shown in Fig. 6. The contribution from changing salinity and the contribution from changing temperature are shown separately. The contribution from changing salinity is calculated using the twenty-first-century averaged temperature and the variable salinity at each depth level and then averaging over the upper 230 m of the water column. A similar calculation using average salinity and variable temperature is done to obtain the temperature contribution.

decrease in density is present along the east coast of Greenland, which is driven by the increased influx of liquid freshwater from the Arctic Ocean through Fram Strait. This relatively low salinity water stays confined to the EGC and appears to have little penetration into the central GIN Seas where deep-water formation occurs. Instead, much of this increased Arctic liquid freshwater exchange is transported by the EGC southward through Denmark Strait. This is consistent with the observations of Curry and Mauritzen (2005) and ice–ocean coupled hindcast modeling experiments (Karcher et al. 2005), which show that most of the recent Fram Strait freshwater transport variations are transported southward with the EGC through Denmark Strait.

At the end of the twenty-first century, reduced Fram Strait ice export contributes to a 0.015-Sv decrease in the freshwater exchange due to net ice melt (melt minus growth) in the GIN Seas. This reduction is approximately 22% of the twenty-first-century Fram Strait ice export reduction. A reduced Denmark Strait freshwater ice transport of about 0.061 Sv over the twenty-first century accounts for the remaining Fram Strait reduction, with much of this resulting in reduced ice melt just south of Denmark Strait (Fig. 16). The decrease in GIN Sea net ice melt is concentrated along the ice edge (Fig. 16) in close proximity to the deep-water formation regions. The GIN Sea meltwater is also redistributed compared to the twentieth-century conditions, with a westward shift in the ice edge resulting in increased ice melt close to Greenland. These changes in ice–ocean freshwater exchange dominate in the changing ocean surface freshwater fluxes in the region. In comparison, the GIN Sea net precipitation increase of 0.005 Sv and river runoff increase of 0.002 Sv over the twenty-first century are quite small and, in the case of $P - E$, less regionally confined. The reduced net ice melt within the GIN Seas contributes to more saline conditions and counteracts surface density changes that result from the increased liquid freshwater transport from the Arctic. An increase in poleward ocean salt transport to the

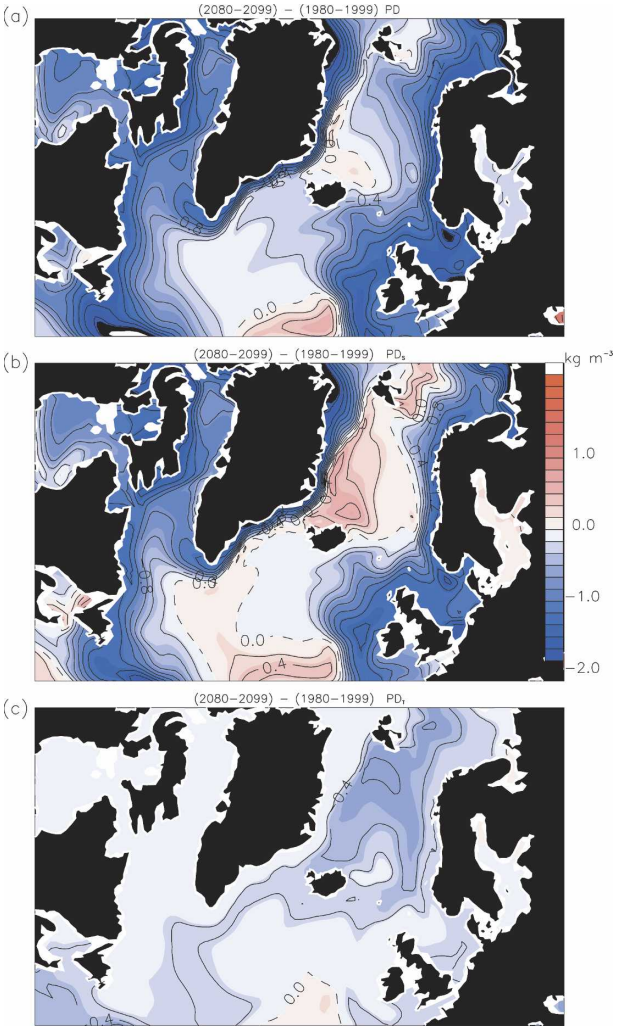

FIG. 15. The change in surface density at the end of the twenty-first century (2080–99) minus the end of the twentieth century (1980–99) for (a) the total change; (b) the change due to variable salinity, computed using 1980–99 average temperature and 2080–99 average salinity; and (c) the change due to variable temperature, computed using 1980–99 average salinity and 2080–99 average temperature. The line contour interval is 0.2 kg m^{-3}, the zero contour is dashed, and negative values are shaded blue.

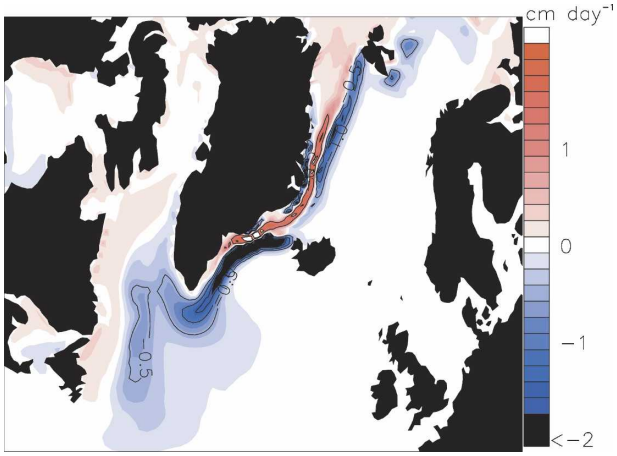

FIG. 16. The change in average net ice melt at the end of the twenty-first century (2080–99) minus the end of the twentieth century (1980–99) in cm day^{-1}. The net melt includes contributions from surface melting, basal melting, lateral melting, basal ice growth, and frazil ice growth.

region from lower latitudes also contributes to increased salinity there. The surface density does decrease over much of the GIN Sea region as a consequence of surface warming, but salinity changes generally have a stabilizing effect.

The maximum mixed layer depths within the GIN Seas give an indication of the deep-water formation there. At the end of the twenty-first century, these are only slightly reduced from those at the end of the twentieth century (Fig. 13). Profiles of ideal age (Fig. 17a) also give information on deep-water formation. Ideal age (Thiele and Sarmiento 1990) is a model tracer that indicates the average time since a parcel of water was exposed to the surface, giving a measure of ocean ventilation. The profiles show that at the end of both the twentieth and twenty-first centuries, the upper 500–600 m of the water column are well ventilated with an ideal age of generally less than 10 yr. This is consistent with the climatological ocean mixed layer depths. Deeper in the water column, the ideal age is considerably older in both the twentieth and twenty-first centuries, indicating that convective events infrequently penetrate to these depths. At these depths, a substantial difference is seen between the end of the twentieth and twenty-first centuries, with the twenty-first century having considerably older waters. These differences are larger than any trends that are present in the preindustrial control integration, indicating that they are robust and a result of the changing climate instead of intrinsic model drift. This suggests that at the end of the twenty-first century there are less frequent convective events penetrating to great depths or older waters being advected into this region at depth. However, the well-ventilated portion of the water column is quite similar between the late twentieth and twenty-first centuries, suggesting that reduced sea ice export and melting help to maintain the deep-water formation in this region.

Our analysis is consistent with the results of Bryan et al. (2006), who examined changes in deep-water formation in transient 1% increasing CO_2 simulations of this model. They found that the GIN Seas maintained a similar rate of deep-water formation in a 4 × CO2 climate but with lighter densities. They attributed this in part to reductions in ice melt within the GIN Seas.

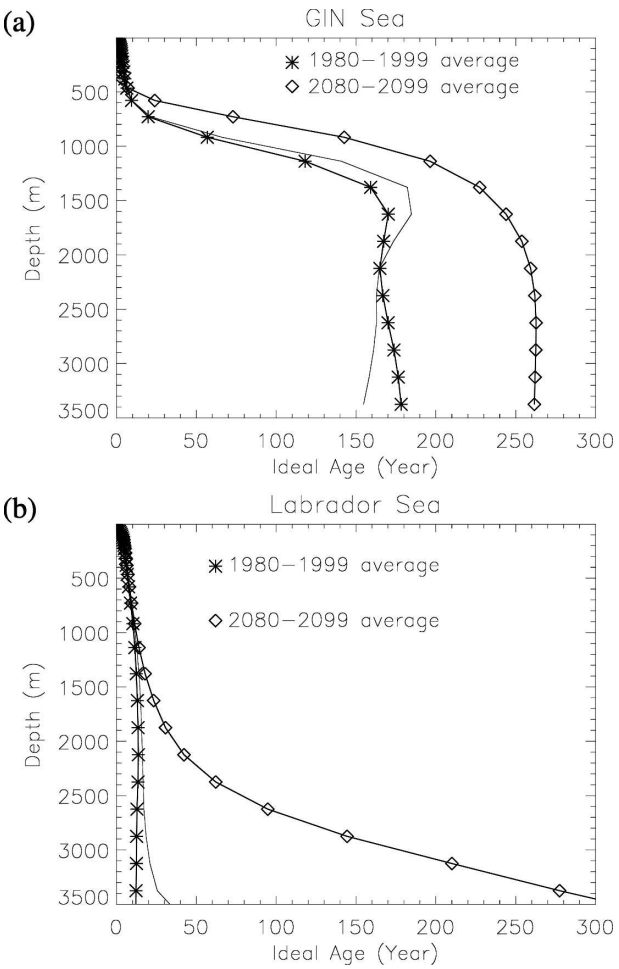

FIG. 17. The profile of ideal age averaged for (a) a GIN Sea deep-water formation region and (b) a Labrador Sea deep-water formation region. The regions are defined as the locations in Fig. 10 within the GIN and Labrador Seas, respectively, where the maximum mixed layer depths are greater than 300 m. The region south of the Greenland–Scotland ridge is not used in either analysis. Shown are values averaged over the end of the twentieth century and over the end of the twenty-first century. The thin solid line shows the 1980–99 profiles modified by the intrinsic model drift, which is assessed from the 1870 control integration.

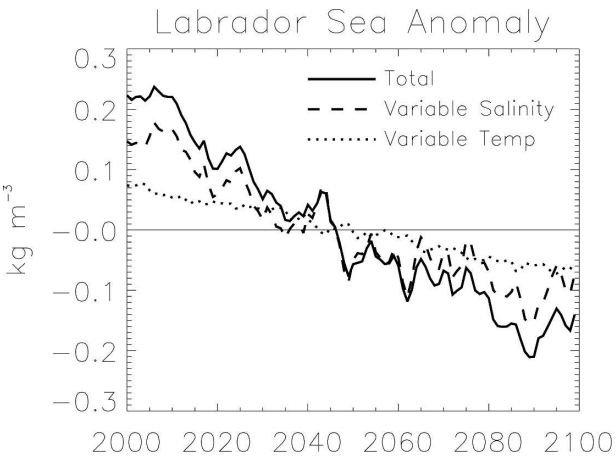

FIG. 18. Same as in Fig. 14, but for the Labrador Sea–Baffin Bay region shown in Fig. 6.

b. The Labrador Sea

Over the twenty-first century, the Labrador Sea receives an increased freshwater flux from the Arctic Ocean through both the Fram Strait liquid water transport, which is advected southward by the EGC into the Labrador Sea, and through increased CAA freshwater transport, which ultimately enters the Labrador Sea from Baffin Bay. There are also reductions in ice transport into the Labrador Sea from both the GIN Seas, much of which has an ultimate Arctic source, and Baffin Bay due to smaller ice growth rates there. The smaller Baffin Bay ice growth freshens the waters and leads to a further increase in the liquid freshwater transport from this region into the Labrador Sea. The increased freshwater fluxes from the Arctic contribute to a decreasing upper-ocean salinity over the twenty-first century in the Labrador Sea–Baffin Bay region (Fig. 18) and counteract reductions in the net ice melt there (Fig. 16). In contrast to the GIN Seas, decreasing salinity is primarily responsible for decreasing density in the Labrador Sea–Baffin Bay with warming temperatures playing a smaller role (Fig. 18).

The simulated Labrador Sea deep-water formation site is displaced southeastward from its observed location. This is likely related to the excessive ice cover in this region (Fig. 1). Additionally, as seen in Fig. 15, although the freshening in the Labrador Sea is more extensive than in the GIN Seas, much of it does stay confined to the boundary and has a reduced effect over the primary deep-water formation site. As suggested by the maximum ocean mixed layer depths at the end of the twenty-first century (Fig. 13) the deep-water formation within the Labrador is decreased. This is also indicated by the ideal age profiles for the Labrador Sea (Fig. 17b). These show that for the 1980–99 average, the Labrador Sea deep-water formation region is well ventilated to considerable depths with the waters throughout the water column to 3500 m having been exposed to the surface within the previous 12 yr. For the 2080–99 average, the waters in the upper 1000 m are also well ventilated. However, deeper in the water column, at the end of the twenty-first century there is considerably less ventilation than for the twentieth-century average, indicating less vigorous deep-water formation.

Both the ocean mixed layer depths and ideal age profiles indicate reduced deep-water formation in the Labrador Sea at the end of the twenty-first century.

However, the influence of increased freshwater transports from the Arctic on this decreasing deep-water formation is not entirely clear. Increased Arctic freshwater transport into this region contributes to reduced salinities and density there, but changes in ocean transports within the Atlantic also likely play an important role. Reductions in ice transport and melting within the Labrador Sea increase the surface salinity but are overwhelmed by other changes that freshen the region.

5. Discussion and conclusions

The simulated Arctic Ocean freshwater budget over the twentieth and twenty-first centuries from CCSM3 integrations has been discussed. In accord with observations, simulated river inputs, net precipitation, and ocean freshwater transport through the Bering Strait freshen the Arctic Ocean and result in fresh polar surface waters. Freshwater is lost from the Arctic by ocean and sea ice transports through Fram Strait and the Canadian Arctic Archipelago (CAA). The magnitude of these various terms compares reasonably well to observed budget estimates (e.g., Aagaard and Carmack 1989; Lammers et al. 2001; Vinje 2001; Woodgate and Aagaard 2005; S06), especially given the considerable uncertainty in many of the observed values, which can differ by more than 50% among different studies, particularly for the ocean flux terms.

Over the twentieth century, the Arctic Ocean receives more freshwater from increased river runoff (particularly from Eurasia) and reduced net ice growth and transport. This contributes to an increased liquid freshwater transport from the Arctic into the North Atlantic through Fram Strait and the CAA. The simulated trends in Eurasian river runoff and Arctic ice volume compare well to observed estimates (Peterson et al. 2002; Rothrock et al. 1999). The simulated trends are significant in the ensemble mean quantities and suggest an intensification of the Arctic freshwater cycle over the twentieth century. However, for individual terms such as net precipitation and river runoff, the interannual variability in individual ensemble members can mask the trends that are present in the ensemble mean for the twentieth century.

Over the twenty-first century, the trends in the freshwater budget terms continue. The maximum 50-yr trend in river runoff is obtained from approximately 2000 to 2050, although this is variable depending on the future emissions scenario that is used to force the model. Increasing precipitation and evaporation are present over both the Arctic Ocean and the watersheds that feed the Arctic. The precipitation changes dominate on the annual average due to increases during the cold season and result in the increased atmosphere and land water flux to the Arctic Ocean.

For solid and liquid freshwater transport from the Arctic, the largest 50-yr trend occurs from approximately 1975 to 2025 for all of the future forcing scenarios that are considered. This is caused in part by large Arctic ice volume decreases and consequent Arctic Ocean freshening that are present over this time period. Ocean circulation changes are also important for the ocean transport trends over the twenty-first century. Through Fram Strait and the CAA an increased mass transport of fresher waters exit the Arctic Ocean over the twenty-first century. In contrast, reductions in mass transport through the Bering Strait counteract the influence of fresher waters entering from the Bering Sea and result in negligible trends in the Bering Strait freshwater import over the twenty-first century.

The increased freshwater transports from the Arctic into the North Atlantic over the twenty-first century freshen both the Nordic and Labrador Seas. This is consistent with the observations of Curry et al. (2003), which show a substantial freshening from the 1950s to the 1990s of Labrador seawater and overflow waters from the Nordic seas. Much of the increased Arctic liquid freshwater transport through Fram Strait stays confined to the East Greenland Current (EGC) and flows southward to the Labrador Sea. Decreasing Fram Strait ice export over the twenty-first century, and consequent reductions in net ice melt within the GIN Seas, results in a decreased ocean surface freshwater flux there. This reduced ice melt contributes to an increase in the surface salinity of these waters, counteracts the density decrease due to warming over the twenty-first century, and helps to maintain deep-water formation in the GIN Seas.

A different picture emerges for the Labrador Sea. Compared to the GIN Seas, the surface ocean density is more influenced by decreasing salinity than increasing temperature over the twenty-first century. These salinity changes are driven in part by increased Arctic freshwater transport through the CAA and within the EGC. Reduced ice transport to this region, some of which has an Arctic source, contributes to reduced ice melt, but the resulting decrease in the ice–ocean freshwater flux is overwhelmed by other processes, and the Labrador Sea freshens. However, while the freshening is more extensive than in the GIN Seas, the largest changes are not present in the deep-water formation regions. Nevertheless, there are considerable decreases in the ocean ventilation and mixed layer depths within the Labrador Sea by the end of the twenty-first century, suggesting a decreased deep-water formation there

Acknowledgments. We thank John Walsh and three anonymous reviewers for helpful comments on this manuscript. Computational facilities have been provided by the National Center for Atmospheric Research (NCAR). Additional coupled sensitivity model integrations were performed by CRIEPI using the Earth Simulator through the international research consortium of CRIEPI, NCAR, and LANL under the Project for Sustainable Coexistence of Human Nature and the Earth of the Japanese Ministry of Education, Culture, Sports, Science and Technology. This work was supported by NSF OPP-0242290.

REFERENCES

Aagaard, K., and E. C. Carmack, 1989: The role of sea ice and fresh water in the Arctic Circulation. *J. Geophys. Res.,* **94,** 14 485–14 498.

——, L. K. Coachman, and E. C. Carmack, 1981: On the halocline of the Arctic Ocean. *Deep-Sea Res.,* **28,** 529–545.

ACIA, 2005: *Arctic Climate Impact Assessment.* Cambridge University Press, 1042 pp.

Arora, V., and G. Boer, 2001: Effects of simulated climate change on the hydrology of major river basins. *J. Geophys. Res.,* **106,** 3335–3348.

Bauch, D., P. Schlosser, and R. D. Fairbanks, 1995: Freshwater balance and the sources of deep and bottom waters in the Arctic Ocean inferred from the distribution of H218O. *Progress in Oceanography,* Vol. 35, Pergamon Press, 53–80.

Belkin, I. M., S. Levitus, J. Antonov, and S. Malmberg, 1998: Great salinity anomalies in the North Atlantic. *Progress in Oceanography,* Vol. 41, Pergamon Press, 1–68.

Bitz, C. M., and W. H. Lipscomb, 1999: An energy-conserving thermodynamic model of sea ice. *J. Geophys. Res.,* **104,** 15 669–15 677.

——, M. M. Holland, M. Eby, and A. J. Weaver, 2001: Simulating the ice-thickness distribution in a coupled climate model. *J. Geophys. Res.,* **106,** 2441–2463.

——, P. R. Gent, R. A. Woodgate, M. M. Holland, and R. Lindsay, 2006: The influence of sea ice on ocean heat uptake in response to increasing CO_2. *J. Climate,* **19,** 2437–2450.

Blindheim, J., 1989: Cascading of Barents Sea bottom water into the Norwegian Sea. *Rapp. P. V. Reun. Cons. Int. Explor. Mer.,* **188,** 49–58.

Bonan, G. B., K. W. Oleson, M. Vertenstein, S. Levis, X. Zeng, Y. Dai, R. E. Dickinson, and Z.-L. Yang, 2002: The land surface climatology of the Community Land Model coupled to the NCAR Community Climate Model. *J. Climate,* **15,** 3123–3149.

Bourke, R. H., and R. P. Garrett, 1987: Sea ice thickness distribution in the Arctic Ocean. *Cold Regions Sci. Technol.,* **13,** 259–280.

Boyd, T. J., M. Steele, R. D. Muench, and J. T. Gunn, 2002: Partial recovery of the Arctic Ocean halocline. *Geophys. Res. Lett.,* **29,** 1657, doi:10.1029/2001GL014047.

Briegleb, B. P., C. M. Bitz, E. C. Hunke, W. H. Lipscomb, M. M. Holland, J. Schramm, and R. E. Moritz, 2004: Scientific description of the sea ice component in the Community Climate System Model, Version Three. NCAR Tech. Note NCAR/TN-463+STR, 70 pp.

Broecker, W. S., 1997: Thermohaline circulation, the Achilles heel of our climate system: Will manmade CO_2 upset the current balance? *Science,* **278,** 1582–1588.

——, D. M. Peteet, and D. Rind, 1985: Does the ocean-atmosphere system have more than one stable mode of operation? *Nature,* **315,** 21–26.

Bryan, F. O., G. Danabasoglu, N. Nakashiki, Y. Yoshida, D.-H. Kim, J. Tsutsui, and S. C. Doney, 2006: Response of the North Atlantic thermohaline circulation and ventilation to increasing carbon dioxide in CCSM3. *J. Climate,* **19,** 2382–2397.

Carmack, E. C., 1990: Large-scale oceanography. *Polar Oceanography: Part A,* W. O. Smith, Ed., Academic Press, 171–222.

——, 2000: The Arctic Ocean's freshwater budget: Sources, sinks and export. *The Freshwater Budget of the Arctic Ocean,* E. L. Lewis et al., Eds., Kluwer Academic, 91–126.

——, R. W. MacDonald, W. Robie, R. G. Perkin, F. A. McLaughlin, and R. J. Pearson, 1995: Evidence for warming of Atlantic water in the southern Canadian Basin of the Arctic Ocean: Results from the Larsen-93 expedition. *Geophys. Res. Lett.,* **22,** 1061–1064.

Cattle, H., and D. Cresswell, 2000: The Arctic Ocean freshwater budget of a climate general circulation model. *The Freshwater Budget of the Arctic Ocean,* E. L. Lewis et al., Eds., Kluwer Academic, 127–140.

Cavalieri, D., C. Parkinson, P. Gloerson, and H. J. Zwally, 1997: Sea ice concentrations from Nimbus-7 SMMR and DMSP SSM/I passive microwave date, June to September 2001. National Snow and Data Center, Boulder, CO, CD-ROM and digital media, updated 2005. [Available online at http://www-sidc.colorado.edu/data/nsidc-0051.html.]

Clark, P. U., N. G. Pisias, T. F. Stocker, and A. J. Weaver, 2002: The role of the thermohaline circulation in abrupt climate change. *Nature,* **415,** 863–869.

Collins, W. D., and Coauthors, 2006a: The Community Climate System Model version 3 (CCSM3). *J. Climate,* **19,** 2122–2143.

——, and Coauthors, 2006b: The formulation and atmospheric simulation of the Community Atmosphere Model version 3 (CAM3). *J. Climate,* **19,** 2144–2161.

Cullather, R. I., D. H. Bromwich, and M. C. Serreze, 2000: The atmospheric hydrologic cycle over the Arctic basin from reanalyses. Part I: Comparison with observations and previous studies. *J. Climate,* **13,** 923–937.

Curry, R., and C. Mauritzen, 2005: Dilution of the northern North Atlantic Ocean in recent decades. *Science,* **208,** 1772–1774.

——, B. Dickson, and I. Yashayaev, 2003: A change in the freshwater balance of the Atlantic Ocean over the past four decades. *Nature,* **426,** 826–829.

Danabasoglu, G., W. G. Large, J. J. Tribbia, P. R. Gent, B. P. Briegleb, and J. C. McWilliams, 2006: Diurnal coupling in the tropical oceans CCSM3. *J. Climate,* **19,** 2347–2365.

Delworth, T., S. Manabe, and R. J. Stouffer, 1997: Multidecadal climate variability in the Greenland Sea and surrounding regions: A coupled model simulation. *Geophys. Res. Lett.,* **24,** 257–264.

Déry, S. J., M. Stieglitz, E. C. McKenna, and E. F. Wood, 2005: Characteristics and trends of river discharge into Hudson, James and Ungava Bays, 1964–2000. *J. Climate,* **18,** 2540–2557.

DeWeaver, E., and C. M. Bitz, 2006: Atmospheric circulation and its effect on Arctic sea ice in CCSM3 simulations at medium and high resolutions. *J. Climate,* **19,** 2415–2436.

Dickinson, R. E., K. W. Oleson, G. Bonan, F. Hoffman, P. Thornton, M. Vertenstein, Z. L. Yang, and X. Zeng, 2006: The

Community Land Model and its climate statistics as a component of the Community Climate System Model. *J. Climate,* **19,** 2302–2324.

Dickson, R. R., J. Meincke, S. A. Malmberg, and A. J. Lee, 1988: Great Salinity Anomaly in the northern North Atlantic 1968–1982. *Progress in Oceanography,* Vol. 20, Pergamon Press, 103–151.

——, and Coauthors, 2000: The Arctic Ocean response to the North Atlantic Oscillation. *J. Climate,* **13,** 2671–2696.

——, S. Dye, M. Karcher, J. Meincke, B. Rudels, and I. Yashayaev, 2006: Current estimates of freshwater flux through Arctic and subarctic seas. *Progress in Oceanography,* in press.

Fowler, C., 2003: Polar pathfinder daily 25 km EASE-Grid sea ice motion vectors. National Snow and Ice Data Center, Boulder, CO, CD-ROM and digital media. [Available online at http://www-nsidc.colorado.edu/data/nsidc-0116.html.]

Gent, P. R., and J. C. McWilliams, 1990: Isopycnal mixing in ocean circulation models. *J. Phys. Oceanogr.,* **20,** 150–155.

Goosse, H., and M. M. Holland, 2005: Mechanisms of decadal Arctic climate variability in the Community Climate System Model, version 2 (CCSM2). *J. Climate,* **18,** 3552–3570.

Grabs, W. E., F. Portmann, and T. de Couet, 2000. Discharge observation networks in Arctic regions: Computation of the river runoff into the Arctic Ocean, its seasonality and variability. *The Freshwater Budget of the Arctic Ocean,* E. L. Lewis, Ed., Kluwer Academic, 249–268.

Grotefendt, K., K. Logemann, D. Quadfasel, and S. Ronski, 1998: Is the Arctic Ocean warming? *J. Geophys. Res.,* **103,** 27 679–27 687.

Hakkinen, S., 1993: An Arctic source for the Great Salinity Anomaly: A simulation of the Arctic ice-ocean system for 1955–1975. *J. Geophys. Res.,* **98,** 16 397–16 410.

Hilmer, M., and T. Jung, 2000: Evidence for a recent change in the link between the North Atlantic Oscillation and Arctic sea ice export. *Geophys. Res. Lett.,* **27,** 989–992.

Holland, M. M., 2003: The North Atlantic Oscillation–Arctic Oscillation in the CCSM2 and its influence on Arctic climate variability. *J. Climate,* **16,** 2767–2781.

——, A. J. Brasket, and A. J. Weaver, 2000: The impact of rising atmospheric CO_2 level on simulated sea ice induced thermohaline circulation variability. *Geophys. Res. Lett.,* **27,** 1519–1522.

——, C. M. Bitz, M. Eby, and A. J. Weaver, 2001: The role of ice–ocean interactions in the variability of the North Atlantic thermohaline circulation. *J. Climate,* **14,** 656–675.

——, ——, E. C. Hunke, W. H. Lipscomb, and J. L. Schramm, 2006: Influence of the sea ice thickness distribution on polar climate in CCSM3. *J. Climate,* **19,** 2398–2414.

Houghton, J. T., Y. Ding, D. J. Griggs, M. Noguer, P. J. van der Linden, X. Dai, K. Maskell, and C. A. Johnson, Eds., 2001: *Climate Change 2001: The Scientific Basis.* Cambridge University Press, 881 pp.

Hunke, E. C., and J. K. Dukowicz, 1997: An elastic–viscous–plastic model for sea ice dynamics. *J. Phys. Oceanogr.,* **27,** 1849–1867.

Karcher, M., R. Gerdes, F. Kauker, C. Koberle, and I. Yashayaev, 2005: Arctic Ocean change heralds North Atlantic freshening. *Geophys. Res. Lett.,* **32,** L21606, doi:10.1029/2005GL023861.

Kattsov, V. M., and J. E. Walsh, 2000: Twentieth-century trends of Arctic precipitation from observational data and a climate model simulation. *J. Climate,* **13,** 1362–1370.

Kleim, N., and D. A. Greenberg, 2003: Diagnostic simulations of the summer circulation in the Canadian Arctic Archipelago. *Atmos.–Ocean,* **41,** 273–289.

Kwok, R., and D. A. Rothrock, 1999: Variability of Fram Strait ice flux and North Atlantic Oscillation. *J. Geophys. Res.,* **104,** 5177–5189.

——, G. F. Cunningham, and S. S. Pang, 2004: Fram Strait sea ice outflow. *J. Geophys. Res.,* **109,** C01009, doi:10.1029/2003JC001785.

——, W. Maslowski, and S. W. Laxon, 2005: On large outflows of Arctic sea ice into the Barents Sea. *Geophys. Res. Lett.,* **32,** L22503, doi:10.1029/2005GL024485.

Lammers, R. B., A. I. Shiklomanov, C. J. Vorosmarty, B. M. Fekete, and B. J. Peterson, 2001: Assessment of contemporary Arctic river runoff based on observational discharge records. *J. Geophys. Res.,* **106,** 3321–3334.

Large, W. G., J. C. McWilliams, and S. C. Doney, 1994: Oceanic vertical mixing: A review and a model with a nonlocal boundary layer parameterization. *Rev. Geophys.,* **32,** 363–403.

——, G. Danabasoglu, S. C. Doney, and J. C. McWilliams, 1997: Sensitivity to surface forcing and boundary layer mixing in a global ocean model: Annual-mean climatology. *J. Phys. Oceanogr.,* **27,** 2418–2447.

Laxon, S., N. Peacock, and D. Smith, 2003: High interannual variability of sea ice thickness in the Arctic region. *Nature,* **425,** 947–950.

Lazier, J. R., 1980: Oceanographic conditions at Ocean Weather Ship Bravo, 1964–1974. *Atmos.–Ocean,* **18,** 227–238.

Lipscomb, W. H., 2001: Remapping the thickness distribution in sea ice models. *J. Geophys. Res.,* **106,** 13 989–14 000.

Manabe, S., and R. J. Stouffer, 1999: The role of thermohaline circulation in climate. *Tellus,* **51A–B,** 91–109.

Mauritzen, C., and S. Hakkinen, 1997: Influence of sea ice on the thermohaline circulation in the Arctic-North Atlantic Ocean. *Geophys. Res. Lett.,* **24,** 3257–3260.

Meehl, G. A., and Coauthors, 2006: Climate change projections for the twenty-first century and climate change commitment in the CCSM3. *J. Climate,* **19,** 2597–2616.

Melling, H., 2000: Exchanges of freshwater through the shallow straits of the North American Arctic. *The Freshwater Budget of the Arctic Ocean,* E. L. Lewis et al., Eds., Kluwer Academic, 479–502.

Meredith, M. P., K. Heywood, P. Dennis, L. Goldson, R. White, E. Fahrback, U. Schauer, and S. Osterhus, 2001: Freshwater fluxes through the western Fram Strait. *Geophys. Res. Lett.,* **28,** 1615–1618.

Miller, J. R., and G. L. Russell, 2000: Projected impact of climate change on the freshwater and salt budgets of the Arctic Ocean by a global climate model. *Geophys. Res. Lett.,* **27,** 1183–1186.

Morison, J., M. Steele, and R. Andersen, 1998: Hydrography of the upper Arctic Ocean measured from the nuclear submarine U.S.S. Pargo. *Deep-Sea Res.,* **45,** 15–38.

Mysak, L. A., and S. A. Venegas, 1998: Decadal climate oscillations in the Arctic: A new feedback loop for atmosphere-ice-ocean interactions. *Geophys. Res. Lett.,* **25,** 3607–3610.

——, K. M. Wright, J. Sedlacek, and M. Eby, 2005: Simulation of sea ice and ocean variability in the Arctic during 1955–2002 with an intermediate complexity model. *Atmos.–Ocean,* **43,** 101–118.

Overland, J. E., M. C. Spillane, and N. N. Soreide, 2004: Integrated analysis of physical and biological panarctic change. *Climate Change,* **63,** 291–322.

Persson, P. O. G., C. W. Fairall, E. L. Andreas, P. S. Guest, and

D. K. Perovich, 2002: Measurements near the Atmospheric Surface Flux Group tower at SHEBA: Near-surface conditions and surface energy budget. *J. Geophys. Res.,* **107,** 8045, doi:10.1029/2000JC000705.

Peterson, B. J., R. M. Holmes, J. W. McClelland, C. J. Vörösmarty, R. B. Lammers, A. I. Shiklomanov, I. A. Shiklomanov, and S. Rahmstorf, 2002: Increasing river discharge to the Arctic Ocean. *Science,* **298,** 2171–2173.

Polyakov, I. V., and Coauthors, 2004: Variability of the intermediate Atlantic water of the Arctic Ocean over the last 100 years. *J. Climate,* **17,** 4485–4497.

Prinsenberg, S. J., and J. Hamilton, 2005: Monitoring the volume, freshwater and heat fluxes passing through Lancaster Sound in the Canadian Arctic Archipelago. *Atmos.–Ocean,* **43,** 1–22.

Proshutinsky, A. Y., and M. A. Johnson, 1997: Two circulation regimes of the wind-driven Arctic Ocean. *J. Geophys. Res.,* **102,** 12 493–12 514.

——, R. H. Bourke, and F. A. McLaughlin, 2002: The role of the Beaufort Gyre in Arctic climate variability: Seasonal to decadal climate scales. *Geophys. Res. Lett.,* **29,** 2100, doi:10.1029/2002GL015847.

Quadfasel, D. A., A. Sy, D. Wells, and A. Tunik, 1991: Warming in the Arctic. *Nature,* **350,** 385.

Rigor, I. G., J. M. Wallace, and R. L. Colony, 2002: Response of sea ice to the Arctic Oscillation. *J. Climate,* **15,** 2648–2663.

Rothrock, D. A., and J. Zhang, 2005: Arctic Ocean sea ice volume: What explains its recent depletion? *J. Geophys. Res.,* **110,** C01002, doi:10.1029/2004JC002282.

——, Y. Yu, and G. A. Maykut, 1999: Thinning of the Arctic sea-ice cover. *Geophys. Res. Lett.,* **26,** 3469–3472.

——, J. Zhang, and Y. Yu, 2003: The Arctic ice thickness anomaly of the 1990s: A consistent view from observations and models. *J. Geophys. Res.,* **108,** 3038, doi:10.1029/2001JC001208.

Serreze, M. C., J. A. Maslanik, R. G. Barry, and T. L. Demaria, 1992: Winter atmospheric circulation in the Arctic basin and possible relationships to the Great Salinity Anomaly in the Northern North Atlantic. *Geophys. Res. Lett.,* **19,** 293–296.

——, and Coauthors, 2000: Observational evidence of recent change in the northern high-latitude environment. *Climate Change,* **46,** 159–207.

——, D. H. Bromwich, M. P. Clark, A. J. Etringer, T. Zhang, and R. Lammers, 2003: Large-scale hydro-climatology of the terrestrial Arctic drainage system. *J. Geophys. Res.,* **108,** 8160, doi:10.1029/2001JD000919.

——, and Coauthors, 2006: The large-scale freshwater cycle of the Arctic. *J. Geophys. Res.,* in press.

Shiklomanov, A. I., T. I. Yakovleva, R. B. Lammers, I. R. Karasev, C. J. Vorosmarty, and E. Linder, 2006: Cold region river discharge uncertainty—Estimates from large Russian rivers. *J. Hydrol.,* **326,** 231–256.

Slonosky, V. C., L. A. Mysak, and J. Derome, 1997: Linking Arctic sea-ice and atmospheric circulation anomalies on interannual and decadal timescales. *Atmos.–Ocean,* **35,** 333–366.

Smith, R., and P. Gent, 2004: Reference manual for the Parallel Ocean Program (POP): Ocean component of the Community Climate System Model (CCSM2.0 and 3.0). Rep. LAUR-02-2484, Los Alamos National Laboratory, Los Alamos, NM, 75 pp.

Steele, M., and T. Boyd, 1998: Retreat of the cold halocline layer in the Arctic ocean. *J. Geophys. Res.,* **103,** 10 419–10 435.

——, and W. Ermold, 2004: Salinity trends on the Siberian shelves. *Geophys. Res. Lett.,* **31,** L24308, doi:10.1029/2004GL021302.

——, D. Thomas, and D. Rothrock, 1996: A simple model study of the Arctic Ocean freshwater balance, 1979–1986. *J. Geophys. Res.,* **101,** 20 833–20 848.

——, R. Morley, and W. Ermold, 2001: PHC: A global ocean hydrography with a high-quality Arctic Ocean. *J. Climate,* **14,** 2079–2087.

Swift, J. H., K. Aagaard, L. Timokhov, and E. G. Nikiforov, 2005: Long-term variability of Arctic Ocean waters: Evidence from a reanalysis of the EWG data set. *J. Geophys. Res.,* **110,** C03012, doi:10.1029/2004JC002312.

Thiele, G., and J. L. Sarmiento, 1990: Tracer dating and ocean ventilation. *J. Geophys. Res.,* **95** (C6), 9377–9391.

Thorndike, A. S., D. S. Rothrock, G. A. Maykut, and R. Colony, 1975: Thickness distribution of sea ice. *J. Geophys. Res.,* **80,** 4501–4513.

Vinje, T., 2001: From Strait ice fluxes and atmospheric circulation: 1950–2000. *J. Climate,* **14,** 3508–3517.

Weatherly, J. W., B. P. Briegleb, W. L. Large, and J. A. Maslanik, 1998: Sea ice and polar climate in the NCAR CSM. *J. Climate,* **11,** 1472–1486.

Weaver, A. J., C. M. Bitz, A. F. Fanning, and M. M. Holland, 1999: Thermohaline circulation: High latitiide phenomena and the difference between the Pacific and Atlantic. *Annu. Rev. Earth Planet. Sci.,* **27,** 231–285.

Woodgate, R. A., and K. Aagaard, 2005: Revising the Bering Strait freshwater flux into the Arctic Ocean. *Geophys. Res. Lett.,* **32,** L02602, doi:10.1029/2004GL021747.

Wu, P., R. Wood, and P. Stott, 2005: Human influence on increasing Arctic river discharges. *Geophys. Res. Lett.,* **32,** L02703, doi:10.1029/2004GL021570.

Zhang, Y., and E. C. Hunke, 2001: Recent Arctic change simulated with a coupled ice-ocean model. *J. Geophys. Res.,* **106,** 4369–4390.